SECURITY CLASSIFICATION OF THIS PAGE (When Data Entered)

REPORT DOCUMENTATION PAGE		READ INSTRUCTIONS BEFORE COMPLETING FORM
1. REPORT NUMBER AFIT/CI/NR 83-84T	2. GOVT ACCESSION NO.	3. RECIPIENT'S CATALOG NUMBER
4. TITLE (and Subtitle) Experimental Measurement of Material Damping For Space Structures in Simulated Zero-G		5. TYPE OF REPORT & PERIOD COVERED THESIS/DISSERTATION
		6. PERFORMING ORG. REPORT NUMBER
7. AUTHOR(s) Raymond Louis Sheen		8. CONTRACT OR GRANT NUMBER(s)
9. PERFORMING ORGANIZATION NAME AND ADDRESS AFIT STUDENT AT: Massachusetts Institute of Technology		10. PROGRAM ELEMENT, PROJECT, TASK AREA & WORK UNIT NUMBERS
11. CONTROLLING OFFICE NAME AND ADDRESS AFIT/NR WPAFB OH 45433		12. REPORT DATE December 1983
		13. NUMBER OF PAGES 120
14. MONITORING AGENCY NAME & ADDRESS(if different from Controlling Office)		15. SECURITY CLASS. (of this report) UNCLASS
		15a. DECLASSIFICATION/DOWNGRADING SCHEDULE

16. DISTRIBUTION STATEMENT (of this Report)

APPROVED FOR PUBLIC RELEASE; DISTRIBUTION UNLIMITED

17. DISTRIBUTION STATEMENT (of the abstract entered in Block 20, if different from Report)

Approved for public release: IAW AFR 190-17.

LYNN E.
D...
I... nal Development
Wright 57 (ATC)

18. SUPPLEMENTARY NOTES

APPROVED FOR PUBLIC RELEASE: IAW AFR 190-17

LYNN E. WOLAVER
Dean for Research and
Professional Development

13 Feb 1984

19. KEY WORDS (Continue on reverse side if necessary and identify by block number)

20. ABSTRACT (Continue on reverse side if necessary and identify by block number)

ATTACHED

DTIC
ELECTE
MAR 21 1984

A

DD FORM 1473 EDITION OF 1 NOV 65 IS OBSOLETE

84 03 20 099

UNCLASS
SECURITY CLASSIFICATION OF THIS PAGE (When Data Entered)

EXPERIMENTAL MEASUREMENT OF MATERIAL DAMPING

FOR SPACE STRUCTURES

IN SIMULATED ZERO-G

by

RAYMOND LOUIS SHEEN

Submitted to the Department of Aeronautical and
Astronautical Engineering on December 23, 1983
in partial fulfillment of the requirement for the
Degree of Master of Science in Aeronautical and
Astronautical Engineering

ABSTRACT

An experimental apparatus for measuring the material damping properties of a beam specimen is described. The apparatus, called Tuneable Excitation Launch Mechanism (TELM) measures the free decay of free-free beams launched into free-fall in a vacuum. Aluminum 2024-T3 specimens are tested with results following the Zener model for specimens with a fundamental free-free frequency above the relaxation frequency. However, specimens with a fundamental free-free frequency below the relaxation frequency show a high degree of stress dependence. Frequency range was 17 Hz to 358 Hz and stress range was 0.5 KSI to 17 KSI. Graphite/epoxy AS1/3501-6 laminates were also tested. For $[0]_8$ laminates, material damping ratio of approximately .00055 was found for frequencies varying from 45 Hz to 237 Hz. The damping was neither stress or frequency dependent. For $[90]_8$ laminates, the damping ratio ranged from .0055 to .0066 as frequency ranged from 42 Hz to 143 Hz. Damping ratios for $[90]_8$ specimens were independent of stress. Metal matrix specimens with graphite fibers, magnesium matrix, and either titanium or magnesium foil were also tested. Damping ratios ranged from .00039 to .00099 depending upon the lay up, frequency, and possibly the stress range involved.

Thesis Supervisor: Dr. Edward F. Crawley

Title: Boeing Assistant Professor of
Aeronautics and Astronautics

AFIT RESEARCH ASSESSMENT

The purpose of this questionnaire is to ascertain the value and/or contribution of research accomplished by students or faculty of the Air Force Institute of Technology (ATC). It would be greatly appreciated if you would complete the following questionnaire and return it to:

AFIT/NR
Wright-Patterson AFB OH 45433

RESEARCH TITLE: __Experimental Measurement of Material Damping for Space Structures in__

__Simulated Zero-G__

AUTHOR: __Raymond Louis Sheen__

RESEARCH ASSESSMENT QUESTIONS:

1. Did this research contribute to a current Air Force project?

( ) a. YES   ( ) b. NO

2. Do you believe this research topic is significant enough that it would have been researched (or contracted) by your organization or another agency if AFIT had not?

( ) a. YES   ( ) b. NO

3. The benefits of AFIT research can often be expressed by the equivalent value that your agency achieved/received by virtue of AFIT performing the research. Can you estimate what this research would have cost if it had been accomplished under contract or if it had been done in-house in terms of manpower and/or dollars?

( ) a. MAN-YEARS _____   ( ) b. $_____

4. Often it is not possible to attach equivalent dollar values to research, although the results of the research may, in fact, be important. Whether or not you were able to establish an equivalent value for this research (3. above), what is your estimate of its significance?

( ) a. HIGHLY   ( ) b. SIGNIFICANT   ( ) c. SLIGHTLY   ( ) d. OF NO
         SIGNIFICANT   SIGNIFICANT   SIGNIFICANCE

5. AFIT welcomes any further comments you may have on the above questions, or any additional details concerning the current application, future potential, or other value of this research. Please use the bottom part of this questionnaire for your statement(s).

NAME _____ GRADE _____ POSITION _____

ORGANIZATION _____ LOCATION _____

STATEMENT(s):

AFIT/NR
WRIGHT-PATTERSON AFB OH 45433

OFFICIAL BUSINESS
PENALTY FOR PRIVATE USE. $300

BUSINESS REPLY MAIL
FIRST CLASS   PERMIT NO. 73236   WASHINGTON D.C.

POSTAGE WILL BE PAID BY ADDRESSEE

AFIT/ DAA
Wright-Patterson AFB OH 45433
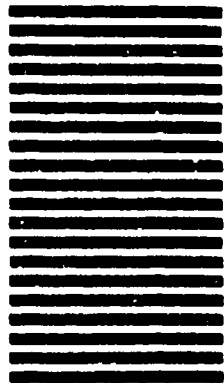
EXPERIMENTAL MEASUREMENT OF MATERIAL DAMPING

FOR SPACE STRUCTURES IN SIMULATED ZERO-G

by

Raymond Louis Sheen

Captain, USAF

DEGREE OF

MASTER OF SCIENCE

at the

MASSACHUSETTS INSTITUTE OF TECHNOLOGY

December 1983

120 pages

84 03 20 099

EXPERIMENTAL MEASUREMENT OF MATERIAL DAMPING

FOR SPACE STRUCTURES IN SIMULATED ZERO-G

by

Raymond Louis Sheen

B.S., United States Air Force Academy

(1977)

SUBMITTED IN PARTIAL FULFILLMENT

OF THE REQUIREMENTS OF THE

DEGREE OF

MASTER OF SCIENCE

at the

MASSACHUSETTS INSTITUTE OF TECHNOLOGY

December 1983

© Massachusetts Institute of Technology 1983

Signature of Author _____
    Department of Aeronautical and Astronautical Engineering
                                    December 23, 1983

Certified by _____
                            Professor Edward F. Crawley
                                    Thesis Supervisor

Accepted by _____
                            Professor Harold Y. Wachman
                    Chairman,Departmental Graduate Committee

The views expressed in this thesis are those of the author and do not reflect the official policy or position of the Department of Defense of the United States Government.

TABLE OF CONTENTS

LIST OF TABLES

6

7

LIST OF FIGURES

9

CHAPTER 1

INTRODUCTION

To characterize the dynamic behavior of any structure, the properties of that structure must be known. These include not only the mass and stiffness, but also the structure's damping characteristics. To determine the damping of a structure, the sources of dissipation must be understood. Sources of dissipation can be divided into two broad categories, external and internal. External sources include active control systems, aeroacoustic effects caused by moving through a fluid, and loss of energy at the supports through either friction or transmission into the supporting structure. Internal sources include friction occurring within the structure and the damping characteristics of the materials used in the structure.

With large flexible space structures the importance of the internal sources of damping is increased. An active control system will probably not be able to control all of the flexible modes of a large space structure. In fact, a closed loop control system can cause higher modes that were initially stable to become unstable; this effect is known as spillover. In the space environment the aeroacoustic and support dissipation mechanisms do not exist. This leaves only the internal forms of damping to dissipate disturbances

10

in the higher modes, and prevent spillover from causing an instability in the structure. Of the forms of internal damping, material damping will be investigated in this study.

There have been many different techniques and geometries which have been used to measure material damping. The three most common techniques are the free decay method, the resonant-dwell method, and the half-power bandwidth method.[3] This study will use the free decay method. Of the different geometries, each has certain advantages and disadvantages. One geometry is to cantilever the specimen.[10,11,12] A problem with this method is ensuring that the specimen stays perfectly fixed at the clamped end. If the specimen does not stay fixed, there will be a damping effect caused by friction at the support. A method often used to reduce this effect is to machine the specimen and support from the same larger piece of material. This is not practical with composite specimens. Similar difficulties exist in the double cantilever.[4].

In order to eliminate fixity uncertainty at the ends, a free-free geometry is often used. The obvious problem with this is supporting the free-free specimen in a gravity field. Usually this is done by supporting the beam at the nodes.[8] However, there is still some effect due to the nodal support. In order to eliminate the requirements for

11

supports, a method of measuring the damping of a free-free specimen in free-fall will be used in this study report. An apparatus that provides this capability exists at MIT and has already been used for previous studies in this field.[1,2]

The materials selected for study were those that are used now are being developed for space applications. Aluminum was chosen since it is used in many structures. Also, since a large experimental data base already exists, it can be used to validate the apparatus. Due to the high strength and low mass, composite materials are already in use on space structures and were therefore chosen for testing. There is a limited data base on the damping characteristics of composite materials. As a third class of potential space structural materials, the damping characteristics of several metal matrix materials, composed of graphite fibers, magnesium matrix and either titanium or magnesium foil, will be examined.

There has already been a significant amount of study done on aluminum by other researchers. Granick and Stern, who used double cantilever specimens tested in both air and vacuum, did not find material damping to be stress dependent in their vacuum results. [4] Also, their data did show damping values slightly higher than those given by the theoretical Zener model. [5] However, they did not test specimens with natural frequencies below the Zener relaxation frequency.

Substantiating this trend, no stress dependence is seen in
the data taken by Mohr.[2] Like Granick and Stern, Mohr found
damping values slightly higher than the Zener curve for
specimens with a frequency above the relaxation frequency.
However, for a single specimen below the relaxation
frequency, the value of damping did not decrease as
suggested by the Zener model. This study will examine
aluminum specimens with frequencies below the Zener
relaxation frequency.

Work done by other researchers with composite materials
is harder to correlate since it is reported in many
different ways and all the information concerning a
particular composite tested is not always provided. Schultz
and Tsai[10] found that damping depended upon fiber
orientation and would transform as the complex part of the
elastic modulus. However, their error between theory and
experimental results ranged from 14% to 37%. Putter,
Buchanan, and Rehfield[12] showed that damping depended upon
temperature, humidity, and ply orientation. Adams and
Bacon[8] demonstrated a very strong correlation between
fiber volume fraction and damping. They also showed a
relationship between beam slenderness ratio and damping,
which correlated well with their theory on composite
damping. Mohr found damping for angle ply laminates to be

13

only slightly dependent on stress and frequency. Mohr
reported reliable data only on the damping of $[\pm 45]_{2s}$
specimens. This study will concentrate on $[0]_8$ and $[90]_8$
graphite/epoxy specimens made from AS1/3501-6 for
correlation with data gathered by Mohr.

CHAPTER 2

EXPERIMENTAL DESIGN

2.1 Description of Apparatus

An experimental apparatus has been developed in the
Space Systems Laboratory (SSL) at the Massachusetts
Institute of Technology to quantify material damping of
candidate specimens for space structures. The apparatus,
called the Tuneable Excitation Launch Mechanism (TELM),
lofts the specimen into free-fall. This eliminates the
effects caused by support and excitation interactions. The
apparatus is contained within a seven foot tall circular
vacuum chamber. The vacuum eliminates any aerodynamic drag
effects. The specimen to be tested is placed on a spring
loaded launcher. The launcher lofts the specimen into
free-fall. During the launch, the acceleration forces cause
the specimen to deflect. Strain gauges on the specimen
measure the deflection as the specimen vibrates. The
apparatus was developed by Vorlicek[1] and Mohr[2] with some
additional modifications made for this study. A complete
analysis of the launch dynamics was done by Mohr.[2]

At the time of Mohr's work the apparatus consisted of a
spring loaded launcher that would loft the specimen into
free-fall. The springs were compressed by hand and an
electromagnet maintained the launcher in a "cocked"

15

position. The amount of compression in the springs and the distance the launcher could travel could be varied. The compression was changed by turning a threaded rod that ran vertically through the launcher and had a steel plate attached to the bottom. The electromagnet held the steel plate when the launcher was cocked. The travel distance was varied by moving a small nut up and down the threaded rod. When the electromagnet released the launcher, the springs forced the launcher up. The adjustable stopper nut would impact a "striker plate" and stop the launcher. (fig 2.1) At the same time the specimen was lofted into free-flight, a terminal block was also lofted upward. This block served as an attachment point for strain gauge wires that came from the specimen. (fig 2.2) The entire apparatus was enclosed by a six foot tall circular vacuum chamber made of plexiglas with an inside diameter of two feet.

Based upon the experiences of Mohr, a number of changes were made in the design of the apparatus. One of the biggest problems encountered was that the chamber had to be opened up between each run to reset the launcher system. The chamber then had to be pumped down again to the proper vacuum before the specimen could be launched. If the entire system could be reset and the launcher settings adjusted from outside the chamber, the time between tests could be reduced. To do this four subassemblies of the TELM had to

16

be modified or developed:

1. The cocking mechanism was modified.

2. The stroke adjustment mechanism was modified.

3. A mechanism to reset the specimen on the launcher following each test was developed.

4. A mechanism to drive the terminal block on a trajectory identical to the specimen was developed.

A subassembly was designed that would automatically compress the springs to recock the launcher. The electromagnet which holds the launcher in the cocked position had previously been fixed to the bottom of the chamber. In the new modified design the electromagnet was mounted on a plate. (fig 2.3) This plate had ball nuts mounted on each end with worm screws running through them allowing for controlled vertical translation of the electromagnet assembly. To reset the system, a small motor would turn the set of worm screws and translate the electromagnet upward until it touched the steel plate on the bottom of the threaded rod. The magnet would then be energized and hold the steel plate that was connected to the launcher by a threaded rod. The worm screws would be energized, drawing the electronmagnet and launcher downward, compressing the springs. The worm screws were stopped at the point when the proper compression was achieved.

17

Another subassembly was designed that would automatically adjust the point at which the launcher would be decelerated so as to achieve the proper launch velocity. The previous adjustment was done by turning by hand the nut that was located on the threaded rod. This nut would impact the "striker plate" that was at a fixed height, and the launcher would stop rapidly, lofting the specimen upward. In the new design, the nut now would impact a hollow shaft that is set in the striker plate. (fig 2.4) This shaft could be moved up and down to set the height where the launcher way decelerated. A DC motor with a gear train turned the shaft. As the shaft turned, it would translate vertically through the striker plate.

A third subassembly was developed that would place the specimen back onto the launcher after a test so that it could be lofted again without the need for the operator to break the vacuum and handle the specimen. The lower section of the plexiglas chamber was replaced by a steel section. This section had two ports through which mechanical arms could be mounted. Each arm was sealed by O-rings at the ports. Each arm had four degrees of freedom and a small claw on the end. These arms were only marginally effective. The arm was difficult to control since the vacuum would constantly try to pull the arm in, and the claws did not have much dexterity. In particular,

18

if the specimen became entangled in the strain gauge wires
the arms could not untangle it. The arms were removed and
the ports sealed after one of the covers for the O-ring
seals cracked and began to leak. For the remainder of the
tests, the vacuum was released following the test and each
specimen manually reset on the launcher.

Another problem encountered by Mohr was that the wires
connecting the strain gauges to the terminal block often
broke. These breaks were usually caused by the terminal
block not matching the trajectory of the specimen. At other
times the magnet holding the terminal block would release
prematurely, snapping the wires. Mohr was using 24 inch
long, 39 gauge, enamel coated wire leading from the terminal
block to the specimen.

To solve the problem of the terminal block not matching
the trajectory of the specimen, a fourth new subassembly was
designed. This subassembly replaced the terminal block with
a smaller block on a wire and pulley system, driven by a DC
motor. (fig 2.5) Because of the high initial torque
required to accelerate the block, followed by an essentially
free-wheeling system, a special motor was needed. When
lofting the lightest weight specimen with the maximum spring
compression, the terminal block would be accelerated to 16.4
feet per second in 13.86 milliseconds. This is an average

19

acceleration of 36.8 "G's". The motor had to have an electrical and mechanical time constant below 13.86 milliseconds, and sufficient torque to accelerate the terminal block pulley system with the required force. A printed circuit pancake motor was chosen that met the performance requirements of the system.

The motor was controlled by an 8 bit microprocessor. The microprocessor would send a velocity profile to the motor controller, which then would match this profile. The micrprocessor also would control the electromagnet that was holding the launcher down. The microprocessor gave the flexibility of changing initial velocity of the terminal block and allowing for a delay between terminal block acceleration and magnet release. This delay was necessary when launching at some of the higher stress settings. The maximum delay used was .01 seconds. A flowchart and copy of the microprocessor program is found in Appendix A.

The problem of the wire breaking was not completely solved, although strain gauge wire reliability was improved. The strain gauge wires were shortened to 18 inches and were soldered onto a four inch section of standard telephone cable at the terminal block end. The terminal block had a two-way female telephone plug mounted

20

on it. One side of the plug received the telephone cable with the strain gauge wires mounted on it. The other side was attached to a ten foot long telephone cable, similr to that found on a standard desk phone. As the terminal ck would travel up and down, this telephone cable would be stretched then would retract. There were fewer problems with wires breaking with this setup. Most breaks occured when the specimen would land and bounce in the bottom of the chamber.

Other changes made to the apparatus were of a fairly minor nature. The vacuum plumbing was redesigned to allow more than one device to be run by the same vacuum pump. A separate release valve was also added. Styrofoam padding was put in the bottom of the chamber to cushion the specimen when it landed. Spacers were designed to be put under the springs so that the amount of compression could be increased. A complete parts list is found in Table 2.1.

2.2 Specimens

The specimens tested were small beams. They varied in length from 5.3 inches to 20 inches and in thickness from .023 inches to .062 inches. All specimens were approximately one inch wide. The specimens were made of aluminum, graphite/epoxy composites, or metal matrix

composites. Aluminum was tested to validate the system and to validate a theoretical model of material damping. The graphite/epoxy and metal matrix were tested to develop a data base on damping values and to validate theoretical models.

A total of 24 specimens were tested during this study. In addition to these tests, the results of tests run by Remy Malan from June to August of 1982 will be reported. A summary of Mohr's work will also be included. All the specimens were instrumented with BLH FDE-25-35-ES strain gauges. These gauges were mounted on the top and bottom surfaces of the specimen at the midpoint. The gauges were connected to the telephone wire by three 18 inch long, 39 gauge, enamel-coated wires.

In an effort to reduce the effect of the strain gauge wires on the damping characteristics, a series of tests were run with the strain gauge wires mounted near the center of the specimen next to the strain gauge, and alternatively with the strain gauge wires mounted at at the location of the node of the first free-free mode shape. (fig 2.6) Depending on the size of the specimen and the type of tests in which the specimen was used, the wires were attached at the specimen center or node as noted.

There were nine aluminum 2024-T3 specimens tested. The dimensions of these specimens are listed in Table 2.2. The specimens were chosen to represent different frequencies along the theoretical Zener curve. The surfaces were sanded and cleaned prior to initial testing to relieve machining stresses. Over the course of collecting data, most of these specimens became slightly scratched. This was due to impacting the side of the chamber or bouncing off portions of the launcher when landing at the end of a test. Specimens Al-1, Al-2, and Al-3 were tested with both center mounted wires and node mounted wires. Specimen Al-4 was tested with center mounted wires. Specimens Al-5, Al-6, Al-7, Al-8, and Al-9 were tested with node mounted wires. In addition to these tests, results of Mohr's aluminum tests will also be reported for comparison.

There were ten graphite/epoxy specimens tested. The dimensions of these specimens are listed in Table 2.3. The specimens were fabricated from AS1/3501-6 pre-preg tape. The lay up sequence and curing cycle were done according to standard TELAC procedures. These procedures are summarized in Appendix B. All of the $[0]_8$ specimens were cut from the same laminate sheet. One of these specimens was then cut to successively shorter lengths to vary the frequency. One $[90]_8$ specimen was used and cut to successively shorter

23

lengths to vary the frequency. The lengths for the $[90]_8$ specimens were chosen to obtain essentially the same frequencies as those tested in the $[0]_8$ specimens. To minimize moisture effects, the specimens were tested within three weeks of initial fabrication and were stored in a zero-humidity chamber following fabrication and between tests. In addition to these tests, a summary of tests done by Mohr on $[\pm45]_{2S}$ graphite/epoxy will be included. The specimens Mohr used are listed in Table 2.4.

There were three metal matrix composites tested. The dimensions of these specimens are listed in Table 2.5. These specimens were provided for test by HR Textron. Details of fabrication are not known.

2.3 Data Collection and Reduction

The general data collection and data reduction systems were the same as those used by Mohr. The strain gauges were mounted on the top and bottom surfaces of each specimen. A complete analysis of the strain gauge bridge circuit is contained in Appendix C. The bridge voltage time history was recorded on a digital oscilloscope and the data points saved on floppy discs. There were 4096 points stored on each test. The time interval between points varied depending upon the frequency of vibration. A minimum of twenty points per cycle was used to insure accurate digital

representation of the waveform.

The data was then transfered to a computer system and digitally filtered. The digitial filter program was based upon an equal ripple routine. The filter was used as a low pass filter to remove higher modes and system noise. The filter parameters were chosen so that the mid-point of the transition band was approximately the same as the mid-poit between the first free-free frequency and the seocnd symmetric, or third free-free, frequency. Other parameters were chosen so as to maintain approximately 75 filter coefficients. Some characteristics of the filtering are a significant phase shift, no frequency shift, and a possible small amplitude gain. This gain was a function of the smoothness and width of the transition band and varied from specimen to specimen. The amplitude gain was never more the 7% of the amplitude and normally less than 2%. Both the unfiltered data and filtered data will be presented in this report. When there is no stress dependency, the filtered data will be used for analysis since it usually provides a smaller standard deviation in damping results. When there is a stress dependency, the unfiltered data will be examined. A comparison of a typical data file that is unfiltered and the same file filtered are found in figures

25

2.7 and 2.8. A copy of this digital filter program is on
file in the SSL at MIT.

The unfiltered and the filtered data was then subjected
to a least-squares curve fit of an exponentially decaying
sinusoid

$$u(t) = A e^{-\zeta \omega t} \sin (\omega t + \phi) + B$$

where A = amplitude

ζ = damping ratio c/c_{cr}

ω = frequency

ϕ = phase angle

B = DC offset

In the fit routine, A, ζ, ω, ϕ, and B are all free
parameters. The program, called LSMARQ, is based on the
work of Marquardt.[15] A copy of the program is on file at
the MIT Information Processing Center.

2.4 Test Procedure

The same test procedure was used for all specimens:

a) Initial compression and stroke adjustments were
determined for the particular specimen and stress level
using the procedure outlined by Crowley and Mohr.[16]

b) The specimen was placed on the launcher and was
checked to ensure it was sitting level.

26

c) The chamber was closed and evacuated to approximately one torr. The chamber was then sealed off from the pump.

d) The plate with the electromagnet was drawn up to the steel plate attached to the launcher, and then drawn back down until the desired compression was obtained.

e) The hollow shaft going through the center of the striker plate was adjusted for the proper stroke.

f) The microprocessor was initialized for the desired rigid body velocity and the desired delay between the terminal block acceleration and magnet release.

g) The oscilloscope was set to collect data.

h) The microprocessor program was executed, accelerating the terminal block and releasing the electromagnet. The electromagnet release pulse was used as the trigger pulse for the oscilloscope.

i) The data was visually inspected on the oscilloscope, and if no problems were noted (broken wires, specimen hitting side of chamber) the data was stored on floppy disc.

j) The atmosphere was readmitted and the procedure was repeated.

k) If specimen trajectory and terminal block trajectory did not match, the compression and stroke adjustments were modified, or the microprocessor program constants were changed.

27

CHAPTER 3

EXPERIMENTAL RESULTS

3.1 Validation and Configuration Tests

The first series of tests were run to ensure that the experimental apparatus was providing data in agreement with previous results. This was done by testing three of the aluminum specimens that Mohr tested.[2] During these tests, these specimens had the strain gauge wires attached at the center of the specimen, as in Mohr's work. The values for Al-1, Al-2 and Al-3 obtained are from the filtered data found in Table 3.1. Mohr's values for these aluminum specimens are given in Table 3.2

In an effort to reduce the possible effects of the strain gauge wires, a series of tests were conducted with the same three specimens, but the strain gauge wires were attached at the location of the node of the first free-free frequency. The results of these tests are found in Table 3.3. Average values for Mohr's tests and the center wire and node wire tests are compared in Table 3.4. The average value was usually lower and the standard deviation usually smaller using node wires. However, for specimen Al-1, the average value and standard deviation were slightly higher with node wires. Following these tests, the decision was

made to use node wires in all tests, except when the mass of the specimen was greater than the mass of specimen Al-1, or when, the same specimen would be tested at different frequencies, causing the node to shift.

3.2 Aluminum Tests

Testing was now done on the remainder of the aluminum specimens. All of these specimens had node wires except specimen Al-4, the twenty inch long specimen. This specimen was the heaviest specimen tested. Since this specimen was the longest tested, it was most likely to hit the side of the chamber during flight and tumble. Experience showed that center mounted wires were less likely to break when the specimen tumbled than node mounted wires. This was also a factor in deciding to use center mounted wires with specimen Al-4. The results of these tests are found in Table 3.5. Specimens Al-5, Al-6, Al-7, and Al-8 have only unfiltered data presented because of the high degree of stress dependence. Specimens Al-4 and Al-9 have filtered data presented since they did not exhibit stress dependence.

Table 3.6 contains data collected by Malan using specimens Al-6 and Al-7. This data was analyzed using Mohr's procedures. This data will be used with the data in Table 3.5 for the analysis of the aluminum specimens.

29

3.3 Graphite/Epoxy Tests

To develop a data base and validate theoretical models for graphite/epoxy composite damping, experimental tests must be conducted on a variety of ply lay ups, frequencies, and stress levels. To remove the effect of shear coupling terms, only symmetric lay ups have been tested initially.[2],[8],[12] Mohr tested $[0]_8$ and $[\pm 45]_{2s}$ specimens. However, his data for the $[0]_8$ specimens was suspect because of specimens curvature and strain gauge debonding. This study tested $[0]_8$ and $[90]_8$ specimens so that, with Mohr's $[\pm 45]_{2s}$, damping data on three different symmetric ply lay ups were available. Each specimen was tested at a variety of stress levels. Different frequency specimens were tested with each lay up. All graphite/epoxy data was filtered.

Tests were run on three different groups of graphite/epoxy specimens. The first group of specimens, $[0]_8$-1, $[0]_8$-2, $[0]_8$-3, and $[0]_8$-4, were tested to determine the eproducibility of results. They were all cut from the same laminate of graphite/epoxy $[0]_8$ and had similar dimensions. The four specimens were all tested at the same stress levels. Specimen $[0]_8$-4 had wires attached at the center, since it was used for frequency tests later. The other three specimens had wires attached at the node. Results of these tests are found in Table 3.7.

30

The next group of tests were using specimens $[0]_8-4$, $[0]_8-5$, $[0]_8-6$, and $[0]_8-7$. These tests were to determine the frequency dependence of the graphite/epoxy $[0]_8$. Specimens $[0]_8-4$, $[0]_8-5$, $[0]_8-6$, and $[0]_8-7$ were formed by cutting specimen to successively shorter lengths, which increased the frequency of vibration. An equal amount was cut from each end of the specimen. This left the strain gauges still mounted at the center of the specimen. Strain gauge wires were also mounted near the center, since the location of the node would change each time the specimen was cut. Results of these tests are found in Table 3.8.

The last group of graphite/epoxy tests were done using specimens $[90]_8-1$, $[90]_8-2$, and $[90]_8-3$. These specimens were manufactured at the same time as the $[0]_8$ graphite/epoxy specimens. The strain gauge wires were attached at the center of each specimen. As with the previous group of tests, the shorter specimens were made by cutting down the longer specimen, thus changing the frequency. Also, the strain gauge wires were attached at the center of each specimen. The lengths of these specimens were chosen so that each would vibrate at approximately the same frequency as one of the $[0]_8$ specimens. The stress level chosen for these specimens was to match the strain level of the corresponding $[0]_8$ specimen's tests. Limitations of the

TELM prevented testing a specimen that matched the frequency of specimen $[0]_8$-7. Results of these tests are found in Table 3.9. The results of Mohr's $[\pm45]_{2S}$ tests on different frequency specimens are found in Table 3.10. These specimens were also obtained by successively cutting down the longest $[\pm45]_{2S}$ specimen.

3.4 Metal Matrix Tests

The two metal matrix specimens with titanium foil, P100/AZ91C/Ti and P55/AZ91C/Ti, were tested with center wires attached. The original plan was to test these specimens at different frequencies by attaching tip weights to the specimen. This was attempted with one of the specimens. However, due to its increased mass, the specimen was damaged by impact with the launcher when it landed. This damage had not occurred when tip weights were not used. No further tests were made with tip weights on any of the specimens.

The metal matrix specimen with magnesium foil had wires attached at the node. This specimen was not as stiff as the other two specimens, therefore, it was tested over a much broader range of strain values.

All of the data reported for these specimens is unfiltered. No stress values are reported for these specimens. The strain values were measured on the outer surfaces of the foil on each of the specimens. Results from these tests are found in Table 3.11.

32

CHAPTER 4

ANALYSIS

In this chapter theoretical models that predict material damping for metals and composites will be examined. The experimental results from Chapter 3 will be compared to these theoretical models to determine the validity of the theory. Aluminum results will be discussed first followed by graphite/epoxy. The damping in metal matrix specimens will be analyzed using both metal and composite models.

4.1 Theoretical Model of Damping in Metals

The earliest models of material damping in metals used a dashpot in parallel with a spring. (fig 4.1) This was known as a "Voight solid".[3,5] However, it was found that this model did not adequately predict the experimental results.[3,5] In particular, the response of the system at high frequency oscillations was incorrect.

A later model had a spring in series with the dashpot, and the two of them in parallel with another spring. (fig 4.2) This model, known as a "standard linear solid", gave much better results.[3,5] This model predicted the damping would be at a peak for a frequency that was a function of the spring and dashpot values, and would decrease for frequencies that were either greater or less than the peak frequency.

33

Zener proposed that the actual mechanism that was occurring was heat flow in the metal. According to Zener, when the material vibrates at low frequencies, the temperature gradient in the specimen remains approximately zero, resulting in a nearly isothermal process. When the material vibrates at high frequencies, the strain in the material oscillates from compression to tension and back again on a time scale shorter than that with which heat can flow through the material resulting in an adiabatic process. So at very low and very high frequencies the total heat flow in the material approaches zero. However, there is an intermediate range of frequencies where heat flows through the material. This heating is a form of energy loss and is a mechanism that causes material damping in metals. The frequency at which maximum heating occurs corresponds to maximum damping and is known as the relaxation frequency.

Zener's development was for body-centered cubic and face-centered cubic materials.[5] He did not address the applicability of this theory for any other crystal structure. However, it may be possible to extend this theory to other crystal structures which have the same atomic packing factor. For example, hexagonal close-packed has an atomic packing factor of .74, which is the same as for face-centered cubic.[6]

A full mathematical development of Zener's theory is found in Appendix D. The final equations used to predict

34

material damping are presented below. One of the advantages
of this theory is that it can predict the material damping
based upon known material properties. According to Zener,
the damping ratio can be expressed by

$$\zeta = \frac{\alpha^2 ET}{2c} \left[\frac{\omega\tau}{1 + (\omega\tau)^2} \right] \qquad (4.1)$$

where

        ζ = damping factor

        α = coefficient of thermal expansion

        E = Young's modulus

        T = absolute temperature

        c = specific heat/unit volume

        ω = frequency of vibration

        τ = relaxation time

and the relaxation time can be found by:

$$\tau = \frac{ch^2}{k\pi^2} \qquad (4.2)$$

where

        h = specimen thickness

        k = thermal conductivity

The inverse of τ is the relaxation frequency, the frequency
where maximum damping will occur. Notice that this theory
predicts that damping is independent of stress level until
the yield stress is reached. Also, the relaxation frequency

35

changes depending upon the thickness of the specimen. This model will be used to correlate with the aluminum specimens. It will also be used in the analysis of the metal matrix composites. The material constants used in these equations were obtained from the MIL Handbook-5C, Vol 1, September 1976.[14]

4.2 Analysis of Damping in Aluminum

The theoretical model proposed by Zener will now be compared to the experimental results. Frequency and stress dependence will be examined. Finally, possible explanations for discrepancies between the theory and experimental results will be discussed.

A plot of all the aluminum specimen's damping ratio as a function of frequency are found in figure 4.3. For frequencies above the relaxation frequency the average values and one standard deviation bars are shown. For frequencies below the relaxation frequency the range of values are shown. The upper limit on these ranges should not be considered as a maximum value of damping, but rather as the value obtained for the maximum level of stress at which the specimens were tested.

The aluminum specimens were observed to have very different behavior depending upon whether their frequencies were above or below the relaxation frequency. All of the specimens tested with a frequency above the relaxation

frequency showed no stress dependence as can be seen by examining Tables 3.1, 3.2, 3.3, and 3.4. The average damping ratio of these specimens followed the Zener curve, which corresponds to results obtained by other researchers.

The specimens with a frequency below the relaxation frequency showed that damping was highly stress dependent and their damping ratios did not follow the Zener curve. A plot of the specimens with a frequency below the relaxation frequency is found in figure 4.4. Points shown on this plot represent an average value of damping ratio over a range of .5 KSI for the specimen represented. This plot shows that the damping ratio was increasing with increasing stress for all four of these specimens. However, the value of damping at very low stresses may be the same for all specimens. The damping ratio is constant or slightly increasing until approximately 8 KSI when the damping begins to increase rapidly with stress.

No research conducted on specimens with a frequency below the relaxation frequency could be found for beams in vacuum. Granick and Stern tested specimens that had frequency as low as 15Hz. However, because of the thickness of these specimens, all frequency values were above the relaxation frequency. Mohr tested one specimen that had a frequency slightly below the relaxation frequency. The damping ratio of this specimen was significantly greater than the predicted Zener value.

37

The reason for this deviation from the Zener theory is not clear. This is the region where Zener said the vibrations would cause isothermal heating through the specimen. Either the heat is being dissipated as it flows from one side of the specimen to the other, or another phenomenon is occuring. The possibility of yielding in the specimen was investigated. Yield stress for aluminum 2024-T3 is 42 KSI. Granick and Stern found that damping ratio increased for aluminum 2024-T4 when tested at stress levels above 35 KSI, but none of the specimens in the current investigation were tested above 20 KSI.

4.3 Theoretical Models of Damping in Composites

Material damping of composite materials cannot be treated in the same way as metals. Composites are neither isotropic nor homogeneous, so properties change depending upon the fiber orientation, volume fraction, and materials used. For this study, three different models of composite damping will be used in the analysis of damping in graphite/epoxy and metal matrix specimens. The results obtained using these methods will then be compared.

For this study, three different models of composite damping will be used in the analysis of damping in graphite/epoxy and metal matrix specimens. The results obtained using these methods will then be compared.

The first model will be a Rule of Mixtures calculation[9]

$$\zeta = V_f \; \zeta_f + V_m \; \zeta_m \qquad (4.3)$$

when

V_f = fiber volume fraction

V_m = matrix volume fraction

ζ_f = fiber damping ratio

ζ_m = matrix damping ratio

In this case, it is assumed that the damping in the matrix is much greater than the damping in the fibers, therefore, the damping can be approximated by

$$\zeta \approx V_m \; \zeta_m \qquad (4.4)$$

This model is independent of fiber orientation and fiber damping characteristics.

The second model was proposed by Hashin[7] and is based upon a transformation of complex moduli. This model assumed a unidirectional composite, although the composite principle axis did not need to be aligned with the specimen longitudinal axis. Hashin also assumed the fibers were

39

brittle and therefore did not contribute to the damping. Because of this, the imaginary part of the fiber modulus is zero. Hashin started with a Rule of Mixtures equation for complex moduli

$$\overset{*}{E}_{11} = E_f \, V_f + \overset{*}{E}_m \, V_m \qquad (4.4)$$

He then separated this into real and imaginary parts

$$E_{11}{}^R = E_f \, V_f + E_m{}^R \, V_m \qquad (4.5)$$

$$E_{11}{}^I = E_m{}^I \, V_m \qquad (4.6)$$

The loss tangent is defined as the imaginary part of the modulus divided by the real part of the modulus, and is proportional to the damping ratio. The loss tangent for the composite is then

$$\tan \delta_E = \frac{E_m{}^I \, V_m}{E_f \, V_f + E_m{}^R \, V_m} \qquad (4.7)$$

Now rearranging terms and substituting in the value of the loss tangent for the matrix

$$\tan \delta_m = \frac{E_m{}^I}{E_m{}^R} \qquad (4.8)$$

40

gives the equation

$$\tan \delta_E = \frac{\tan \delta_m}{\frac{E_f V_f}{E_m V_m} + 1} \qquad (4.9)$$

Since the loss tangent is proportional to the damping ratio, we have an expression for the damping ratio of the composite:

$$\zeta = \frac{\zeta_m}{\frac{E_f V_f}{E_m V_m} + 1} \qquad (4.10)$$

where

ζ_m = the damping ratio of the matrix

E_f = Fiber axial Young's modulus

E_m = Matrix Young's modulus

v_f = fiber volume fraction

v_m = matrix volume fraction

The third model was proposed by Adams and Bacon and is based upon a combination of Hashin's equation using the complex moduli and the shear stress caused by flexure.[8] This model is also restricted to unidirectional composites. In this model the specific damping capacity of a composite in the sum of the axial damping capacity, found using Hashin'sequation, and the shear damping capacity. The shear damping capacity is the result of the energy dissipated in each cycle because of shear. A complete derivation of this shear damping capacity is found in the reference by Adams and Bacon[8].

41

The damping capacity is proportional to the damping ratio, so the equation for the shear damping ratio is:

$$\zeta_s = \frac{\zeta_{12} \int_0^{L/2} \left(\frac{\partial^3 w}{\partial x^3}\right)^2 dx}{\int_0^{L/2} \left(\frac{\partial^3 w}{\partial x^3}\right)^2 dx + \frac{10 \, G_{12}}{E_{11} \, h^2} \int_0^{L/2} \left(\frac{\partial^2 w}{\partial x^2}\right)^2 dx} \qquad (4.11)$$

w = mode shape

h = specimen thickness

L = specimen length

E_{11} = Composite Young's modulus along primary axis

G_{12} = Composite shear modulus

ζ_{12} = Longitudinal shear damping ratio

4.4 Analysis of Damping in Graphite/Epoxy

When analyzing the damping in graphite/epoxy, there were a series of questions to be addressed. The first question concerned the reproducibility of results. Next were the questions of stress, frequency, and fiber orientation dependence of damping. Finally the validity of the theoretical models was to be checked. Each of these questions will be discussed, and where applicable, the resultswill be compared to that of other researchers. All tests were performed at room temperature and near zero moisture content to remove any dependence of damping on these factors.

42

The first question dealt with the reproducibility of the results. When composites are made there are often tiny voids, broken fibers, and misaligned fibers that can possibily affect the characteristics of a specimen.[9] To investigate the effects these non-uniformities might have on damping, four specimens were constructed to be as similar as possible, $[0]_8$-1, $[0]_8$-2, $[0]_8$-3, and $[0]_8$-4. These specimens were cut from the same sheet of laminate with nearly identical dimensions. Therefore, four specimens had nearly the same frequency of vibration. In all four specimens, the damping ratio was not dependent upon stress. The average values and the standard deviation were approximately the same for all four specimens, as can be seen in Table 4.1. Although the difference between the highest value of damping ratio and lowest value of damping ratio is .00013, or 25% of the damping ratio; the largest standard deviation is only .00009, or 18% of the damping ratio.

The next questions was to determine frequency dependence of the damping ratio in $[0]_8$ graphite/epoxy. Specimen $[0]_8$-4 was cut to successively shorter lengths, thereby changing the frequency but keeping the volume fraction, width, thickness, and internal non-uniformities of the specimen constant. There was little change in the damping ratio with frequency as can be seen in Figure 4.5.

43

The average value of damping ratio along with a one standard deviation bar, and the highest and lowest value obtained for each speciman are plotted in figure 4.5. In each of these tests of $[0]_8$ specimens, damping ratio was independent of stress level. Putter, Buchanan, and Rehfield found a value of $\zeta = .00062$ for their $[0]_{12}$ specimens of graphite/epoxy which compares very well with these values.[12]

Another set of tests of material damping as a function of frequency were conducted with $[90]_8$ graphite/epoxy. Again the longest specimen was cut to successively shorter lengths. As can be seen in figure 4.6, material damping does depend on frequency in the $[90]_8$ specimens. Increased frequency leads to increased damping. However, again there was no stress dependence for the damping ratio of a particular frequency specimen.

The r t question was whether the damping ratio depended on fiber orientation. The results of the $[0]_8$ tests and the $[90]_8$ tests will be used along with tests conducted by Mohr on $[\pm 45]_{2S}$ specimens.[2] There are currently few theories that predict damping for other than a unidirectional composite. Schultz and Tsai had studied the relationship of fiber orientation, but limited themselves to unidirectional lay ups. By using Mohr's $[\pm 45]_{2S}$ data, this study will be using symmetric lay ups. A plot of Mohr's data is found in figure 4.7 for four frequencies. As

44

can be seen by comparing figures 4.5, 4.6 and 4.7, there is an order of magnitude difference in damping ratios between the $[0]_8$ and the other two orientations for the frequency and stress ranges tested. Notice that the stress ranges tested in the $[90]_8$ specimens were set to correspond with the strain levels tested in the $[0]_8$ specimens. The values for three fiber orientations at approximately the same frequency are shown in figure 4.8.

The final question was how well does theory match the experimental results. In all three theories, the value of damping for the matrix is needed. Unfortunately, the manufacturer of the pre-preg tape used in the graphite/epoxy specimens did not have any information on the damping characteristics of the epoxy. In order to still test the theoretical models in at least a limited fashion, the models were used to back calculate a value for the matrix damping, assuming the fiber contributed no damping. The values from each specimen were then compared to each other to see if the values of matrix damping were approximately the same value. Consistent values of matrix damping caluculated from different tests in this manner would be a necessary condition for verification of the analytic model. Since these theories are all limited to unidirectional composites, the $[\pm 45]_{2s}$ data will not be used.

45

Applying the three theories of damping in unidirectional laminates to the damping values for $[0]_8$-1, $[0]_8$-2, $[0]_8$-3, and $[0]_8$-4 yields back-calculated values for matrix damping for each specimen and theory. These values and their average are found in Table 4.2 The average will be used as a reference value for comparison with other test results.

Values of matrix damping can also be found from the $[0]_8$ specimens of differing frequency, as shown in Table 4.3. When applying the three theories for composite damping, the values obtained are all close to the reference values for the appropriate theory as derived from the specimens of similar geometry. There is a trend in all three theories towards slightly lower values of matrix damping with higher frequency.

Finally the $[90]_8$ frequency specimens are used to obtain matrix damping values (Table 4.4). The results are significantly different from the reference values of Table 4.2. Not surprisingly the values for matrix damping are increasing with frequency just as the specimen damping value did. The rule of mixtures method gave values that are an order of magnitude different from the referenceaverage values. The other two theories gave values below, but within 20% of, the reference average values. Also, the effect of shear is virtually unnoticable in these specimens. Therefore there is no difference in the values for the two

46

theories using complex moduli, one which accounts for shear damping and the other which omits this effect.

In an effort to determine how accurately these theories predict damping, it is interesting to compare the matrix damping back-calculated from theory with actual measured values of damping for other epoxies. Georgi quotes a matrix damping value of .011 and Schultz and Tsai have values of .0162 and .0193 for the frequency range that was tested in their experiments. These values are lower than the values obtained here. However, since those values are for a different epoxy, definite conclusions can not be drawn.

One other significant result is that the real part of the composite modulus is significantly below the modulus obtained from static tensile testing. This is in agreement with results obtained by Turner[13]. By using the frequency of vibration, specimen dimensions, and mass, the real part of the modulus can be back-calculated using the relation

$$E = \frac{M\ L^3\ \omega^2}{(22.373)^2 I} \qquad (4.12)$$

where

> M = mass
>
> L = length
>
> ω = frequency of first free-free mode
>
> I = moment of Inertia

The calculated values of the real part of the modulus are found in Table 4.5.

47

4.5 Analysis of Damping of Metal Matrix Material

The data for damping in metal matrix material will be examined to determine what trends are evident, and will be compared with the theoretical models discussed in this report.

The data for the two specimens with titanium foil, P100/AZ91C/Ti and P55/AZ91C/Ti, showed no stress level dependency. This is shown in Table 3.11. However, the strain range involved was fairly small due to limitations of the TELM. The specimen with magnesium foil, P100/AZ91C/Mg, showed a very slight stress dependence. This was over a strain range of 36 μs to 176 μs as shown in Table 3.11. Stress values are not reported because the stress distribution through the metal matrix is not known. Frequency dependence could not be tested for any of these specimens since only one specimen was provided, and its geometry could not be altered. The order of magnitude of the damping ratio for all of these specimens is the same as both aluminum and $[0]_8$ graphite/epoxy.

The damping ratios for all of the specimens were compared to theoretical Zener values for magnesium AZ91C, which is the matrix being used. This was done by assuming the specimens are made entirely of magnesium, but have the same dimensions as the ones tested. The theoretical and the actual damping ratios for each specimen are plotted in

figure 4.9.   The two specimens with a frequency above the relaxation frequency, P100/AZ91C/Ti and P55/AZ91C/Ti, exhibit the same characteristics that aluminum showed.   That is no strain dependence, and a value slightly above Zener's predicted value.   The specimen with a frequency below the relaxation frequency, P100/AZ91C/Mg, does not behave the way aluminum did.   The average value is slightly below the predicted Zener value, but the lowest extreme is well below the Zener model value.   The much larger standard deviation for this specimen can be at least partly attributed to the fact that this specimen was the lightest specimen tested. Therefore, any experiement interference due to the apparatus would probably have a greater effect on this specimen than on any other.   It should be noted that the Zener theory is based on a crystal structure of body-centered cubic or face-centered cubic, and magnesium is hexagonal close packed.   Therefore, the Zener model may not be appropriate for magnesium.

To adequately compare the experimental results with theoretical models for composite damping, more information on the specimens is required.   In particular, volume fraction and shear modulus are needed, and the effect of the foil must be determined.   Since no details on the manufacture of the metal matrix specimens were available, some assumptions were made.   First, the only specimen used for theoretical validation was the specimen with the

tagnesium foil, P100/AZ91C/Mg. The specimens with titanium foil involved too many unknown quantities, whereas the specimen with the magnesium foil was at least limited to just two materials, graphite fibers and magnesium matrix and foil. The fiber volume fraction of this specimen was estimated at .15 using a rule of mixtures calculation on the modulus

$$E_{11} = E_f V_f + E_m V_m \qquad (4.13)$$

where E_{11} was back-calculated from the frequency of vibration. The specimen was assumed to be unidirectional with the composite principle axis parallel to the specimen longitudinal axis. Finally, the shear modulus was assumed equal to that of the magnesium shear modulus.

The results of using the theoretical models of composite damping are found in Table 4.6. The value used for the matrix damping was the theoretical Zener value. The rule of mixtures calculation is close to the experimental results, while the complex moduli and shear effects theories are significantly greater. This difference could be due to the theory leaving out some effect, the value for magnesium damping being wrong, or characteristics of the composite assumed for the calculations being in error.

50

CHAPTER 5

CONCLUSIONS AND RECOMMENDATIONS

5.1 Conclusions

The experimental data leads to the following
conclusions:

1. Material damping in aluminum 2024-T3 follows the
Zener curve for frequencies above the relaxation frequency.
In this region the damping is independent of stress level up
to approximately 16 KSI, or 1500 μs.

2. For frequencies below the relaxation frequency,
aluminum 2024-T3 does not follow the Zener curve. There is
a strong dependence on stress levels as low as 8 KSI, or
750 μs, and a slight frequency dependence. There appears to
be a lower bound in the damping that is approximately the
same as the maximum value for damping that the Zener model
predicts.

3. Material damping in graphite/epoxy $[0]_8$ was found
to be independent of stress and independent of frequency.
Damping ratios ranged from .049% to .064% with an average of
.056%. The stress range tested was from 0.3 KSI to
12.8 KSI, 20 μs to 775 μs, and the frequency range was from
45 Hz to 237 Hz.

4. Material damping in graphite/epoxy $[90]_8$ was
independent of stress and slightly dependent on frequency,

increasing with increasing frequency. Damping ratios ranging from .55% to .66% were obtained. The stress ranges were from 0.009 KSI to 0.84 KSI, 7 µs to 675 µs, and the frequency range was 43 Hz to 143 Hz.

5. Dynamic modulus for graphite/epoxy $[0]_8$ was approximately 15% lower than static modulus. Dynamic modulus for graphite/epoxy $[90]_8$ was also approximately 15% lower than static modulus.

6. Hashin's theory for damping in unidirectional composites gives consistent values for matrix damping when applied to graphite/epoxy $[0]_8$ and $[90]_8$. No statement can be made concerning whether the addition of shear effects is beneficial or not.

7. Damping ratio for metal matrix P100/AZ91C/Ti is independent of strain over the range 17 µs to 47 µs. A value of .039% damping ratio was found at a frequency of 494 Hz.

8. Damping ratio for metal matrix P55/AZ91C/Ti is independent of strain over the range 37 µs to 61 µs. A value of .039% damping ratio was found at a frequency of 401 Hz.

9. Damping ratio for metal matrix P100/AZ91C/Mg may be slightly dependent on strain over the range 36 µs to 176 µs

52

An average value of .099% was found at a frequency of 138 Hz.

5.2 Recommendations

1. Further testing should be done on aluminum specimens with frequencies below the Zener relaxation frequency. Stress ranges from near zero to near yield should be investigated.

2. Other metals with cubic crystal structure should be tested to determine whether they follow the Zener curve.

3. Further testing should be done with unidirectional graphite/epoxy specimens that have a lower slenderness ratio to determine the validity of the use of shear effects when predicting the composite damping ratio.

4. The value of the damping ratio of the epoxy resin should be determined. With this value the theories involving complex moduli could be validated against experimental data.

5. A theoretical model for predicting composite damping that is valid for other than unidirectional composites should be developed.

6. Further study of metal matrix composites should be done to increase the data base and to determine if the damping characteristics should be modeled as those of a pure metal or those of a composite.

LIST OF REFERENCES

1. Vorlicek, P.L., "Material Damping of Aluminum and Graphite/Epoxy in a Simulated Zero-Gravity Environment," M.I.T. Space Systems Laboratory #13-81, January 1981.

2. Mohr, D.G. and Crawley, E.F., "Experimental Measurements of Material Damping of Aluminum and Graphite/Epoxy in Free-Fall with Tuneable Excitation," M.I.T. Space Systems Laboratory #11-82, June 1982.

3. Bert, C.W., "Material Damping: An Introductory Review of Mathematical Models, Measures and Experimental Techniques," Journal of Sound and Vibration, (1973), 29(2), pps 129-153.

4. Granick, N. and Stern, J.E., "Material Damping of Aluminum by a Resonant-Dwell Technique," NASA TN D-2893, August 1965.

5. Zener, C.M., Elasticity and Anelasticity of Metals, University of Chicago Press, Chicago, 1948.

6. Van Vlack, L.H., Elements of Materials Science and Engineering, Addison-Wesley Publishing Company, Reading, MA, 1975.

7. Hashin, Z., "Complex Moduli of Viscoelastic Composites-II. Fiber Reinforced Materials," Int. J. Solids and Structures, Vol. 6, 1970.

8. Adams, R.D. and Bacon, D.G.C., "The Dynamic Properties of Unidirectional Fibre Reinforced Composites in Flexure and Torsion," J. Composite Materials, Vol. 7, January 1973.

9. Ashton, J.E., Halpin, J.C. and Petit, P.H., Primer on Composite Materials: Analysis, Technomic Publishing Company, Westport, CT, 1969.

10. Schultz, A.B. and Tsai, S.W., "Dynamic Moduli and Damping Ratios in Fiber-Reinforced Composites," J. Composite Materials, Vol. 2, July 1963.

11. Georgi, H., "Dynamic Damping Investigations on Composites," AGARD Conference, Structures and Material Panel Specialists Meeting on Damping Effects in Aerospace Structures, Williamsburg, VA, April 1979.

12. Putter, S., Buchanan, D.L., Rehfield, L.W., "Influence of Frequency and Environmental Conditions on Dynamic Behavior of Graphite/Epoxy Composites," in Composite Materials: Testing and Design (Sixth Conference), ASTM STP 787, I.M. Daniel, Editor, ASTM, 1982, pp 414-424.

13. Turner, M.D., "Comparison of Static and Dynamic Test Methods for Determining the Stiffness Properties of Graphite/Epoxy Laminates,"S.M. Thesis, M.I.T., Cambridge, MA, June 1979.

14. Military Standardization Handbook, Metallic Materials and Elements for Aerospace Vehicle Structures, MIL-Hdbk-5C, Vol. 1, September 1976.

15. Marquardt, D.W., "An Algorithm for Least-Squares Estimation of Nonlinear Parameters," Journal of the Society for Industrial and Applied Mathematics, Vol. 11, No. 2, June 1963.

16. Crowley, E.F. and Mohr, D.G., "Experimental Measurements of Material Damping in Free Fall with Tuneable Excitation," Presented at AIAA/ASME/ASCE/AHS Structures, Structural Dynamics and Materials Conference, Paper No. 83-0858-CP, Tahoe, NV, May 1983, will be published in AIAA Journal.

TABLE 2.1

EQUIPMENT LIST

Device	Manufacturer	Model Number
Vacuum Pump	Kinney	KD-30
Vacuum Gauge	Stokes	276AA-Lo7
Microprocessor	S.D. Systems	Z80 Starter Kit
Electromagnet	Edmund Scientific	71936
D. C. Motors	Globe Industries Photocircuits Barber Coleman	SO 9667 U9M4H/U6 CYQM 43210-41-5
Tachometer	PMI	U6T
Controller	ORD, Inc.	MP-1
Power Supplies	Kepco Power/Mate Power/Mate Heathkit	ABC 15-1 M PT - 15A BPA - 10 D
Battery (for strain gauge excitation)	Globe	GC626
Strain Gauges	BLH Electronics	FDE-25-35-ES
Oscilloscope	Nicolet Instruments	206

TABLE 2.2

ALUMINUM SPECIMENS

SPECIMEN	LENGTH IN	WIDTH IN	THICKNESS IN	MASS SLUGS (10^{-3})
Al-1 *	18.00	1.00	.062	3.409
Al-2 *	14.00	1.00	.062	2.652
Al-3 *	6.00	1.00	.062	1.136
Al-4	20.00	1.00	.062	3.789
Al-5	18.94	1.00	.031	1.794
Al-6 **	14.00	1.00	.031	1.326
Al-7 **	10.00	1.00	.031	0.947
Al-8	8.00	1.00	.031	0.758
Al-9	6.00	1.00	.031	0.568
Al-10***	10.00	1.00	.061	1.894

* specimens also tested by Mohr
** specimens also tested by Malan
*** specimen tested only by Mohr

TABLE 2.3

GRAPHITE/EPOXY SPECIMENS

SPECIMEN	LENGTH IN	WIDTH IN	THICKNESS IN	MASS SLUGS (10^{-3})
$[0]_8$-1	17.75	1.01	.042	1.297
$[0]_8$-2	17.78	0.99	.041	1.245
$[0]_8$-3	17.75	1.01	.042	1.291
$[0]_8$-4	17.75	1.00	.043	1.301
$[0]_8$-5 *	13.88	1.00	.043	1.020
$[0]_8$-6 *	10.00	1.00	.043	0.735
$[0]_8$-7 *	7.88	1.00	.043	0.579
$[90]_8$-1	9.66	1.00	.041	0.683
$[90]_8$-2 **	7.34	1.00	.041	0.519
$[90]_8$-3 **	5.31	1.00	.041	0.375

* specimen [0]8-4 cut to a shorter length
** specimen [90]8-1 cut to a shorter length

TABLE 2.4

MOHR'S $[\pm 45]_{2S}$ GRAPHITE/EPOXY SPECIMENS[2]

mass/unit length = 7.331×10^{-5} slugs/in.

Specimen	Length (in)	Width (in)	Thickness (in)
$[\pm 45]_{2S}$-1	18.00	0.99	.041
$[\pm 45]_{2S}$-2*	14.12	0.99	.041
$[\pm 45]_{2S}$-3*	10.00	0.99	.041
$[\pm 45]_{2S}$-4*	5.97	0.99	.041

*Specimen $[\pm 45]_{2S}$-1 cut to a shorter length

TABLE 2.5

METAL MATRIX SPECIMENS

SPECIMEN	LENGTH IN	WIDTH IN	THICKNESS IN	MASS SLUGS (10^{-3})
P100/AZ91C/Ti	6.00	1.00	.044	0.624
P55/AZ91C/Ti	6.10	1.00	.045	0.630
P100/AZ91C/Mg	8.00	0.96	.023	0.363

58

TABLE 3.1

DAMPING IN ALUMINUM SPECIMENS WITH CENTER WIRE ATTACHMENT
(VALIDATION TESTS)

Specimen	Frequency rad/sec	Damping Ratio ζ	Strain 10^{-6}	Stress KSI
Al-1	248.5	.001222	1060	11.1
Al-1	248.5	.001226	1078	11.3
Al-1	248.3	.001191	1078	11.3
Al-1	248.3	.001210	1084	11.4
Al-1	248.3	.001201	1127	11.8
Al-1	248.2	.001257	1144	12.0
Al-1	248.4	.001273	1148	12.1
Al-1	248.2	.001264	1150	12.1
Al-1	248.2	.001184	1195	12.5
Al-1	248.0	.001293	1215	12.8
Al-1	248.2	.001282	1221	12.8
Al-1	247.9	.001094	1227	12.9
Al-1	247.9	.001241	1230	12.9
Al-1	247.9	.001210	1282	13.5
Al-1	248.0	.001235	1289	13.5
Al-1	247.7	.001323	1310	13.8
Al-1	247.7	.001203	1362	14.3
Al-1	247.8	.001227	1368	14.4
Al-1	247.4	.001145	1399	14.7
Al-1	247.5	.001183	1448	15.2
Al-1	247.6	.001245	1458	15.3
Al-2	412.3	.0009700	174	1.8
Al-2	412.2	.0011247	175	1.8
Al-2	412.2	.0009872	175	1.8
Al-2	412.3	.0009432	176	1.8
Al-2	412.2	.0010359	190	2.0
Al-2	412.3	.0009261	190	2.0
Al-2	412.3	.0009631	192	2.0
Al-2	412.3	.0011157	193	2.0
Al-2	412.2	.0010474	207	2.2
Al-2	412.3	.0010089	211	2.2
Al-2	412.1	.0011759	310	3.3
Al-2	412.2	.0012268	314	3.3
Al-2	412.2	.0010622	329	3.5
Al-2	412.2	.0010060	341	3.6
Al-2	412.1	.0011863	342	3.6
Al-2	412.2	.0011916	348	3.6
Al-2	412.2	.0010756	361	3.8
Al-2	412.2	.0009992	371	3.9
Al-2	412.1	.0011543	378	4.0
Al-2	412.2	.0011888	384	4.0
Al-2	412.2	.0011510	395	4.1
Al-2	412.2	.0009927	403	4.2

TABLE 3.1 (Continued)

DAMPING IN ALUMINUM SPECIMENS WITH CENTER WIRE ATTACHMENT
(VALIDATION TESTS)

Specimen	Frequency rad/sec	Damping Ratio ζ	Strain 10^{-6}	Stress KSI
Al-3	2247	.0004349	18.9	.20
Al-3	2247	.0004690	19.0	.20
Al-3	2246	.0003677	20.3	.21
Al-3	2246	.0005095	20.4	.21
Al-3	2246	.0005404	21.7	.23
Al-3	2247	.0002231	22.0	.23
Al-3	2246	.0002529	22.2	.23
Al-3	2246	.0006915	24.1	.25
Al-3	2247	.0004535	26.5	.28
Al-3	2247	.0005094	31.0	.33
Al-3	2247	.0004707	31.5	.33
Al-3	2247	.0005079	33.6	.35
Al-3	2247	.0004353	35.6	.37
Al-3	2247	.0003631	37.0	.39
Al-3	2247	.0004720	40.7	.43
Al-3	2246	.0003275	44.5	.47
Al-3	2246	.0003905	48.2	.51

60

TABLE 3.2

SUMMARY OF DAMPING IN ALUMINUM SPECIMENS WITH CENTER WIRE ATTACHED AS REPORTED BY MOHR[2]

Specimen	Frequency rad/sec	Damping Ratio ζ	Stress KSI
Al-1	248.8	.00120209	13.94
		.00111602	12.74
		.00118282	11.58
		.00111504	7.73
		.00111425	7.08
		.00112549	6.50
Al-2	411.4	.00105498	18.09
		.00103198	15.82
		.00102788	13.70
		.00101322	6.99
		.00103550	6.13
		.00106383	5.32
		.00104420	5.07
		.00106423	4.39
		.00108520	3.89
Al-3	2246	.00037952	2.17
		.00039311	1.95
		.00029632	1.86
		.00030515	1.77
		.00030319	1.72
		.00034681	1.58
		.00025401	.93
		.00031441	.89
		.00031991	.84
Al-10	807.2	.00069232	9.03
		.00065044	7.62
		.00063527	6.54
		.00059834	3.71
		.00063423	3.25
		.00067457	2.85
		.00069104	1.26
		.00062124	1.08
		.00062533	.94

TABLE 3.3

DAMPING OF ALUMINUM SPECIMENS WITH NODE WIRE ATTACHMENT

Specimen	Frequency rad/sec	Damping Ratio ζ	Strain 10^{-6}	Stress KSI
Al-1	249.1	.0012501	558	5.9
Al-1	249.0	.0011928	580	6.1
Al-1	249.0	.0012324	581	6.1
Al-1	249.3	.0012643	591	6.2
Al-1	249.1	.0012541	594	6.2
Al-1	249.0	.0012205	616	6.5
Al-1	249.0	.0012485	618	6.5
Al-1	249.3	.0012421	629	6.6
Al-1	249.1	.0013190	632	6.6
Al-1	249.0	.0012002	654	6.9
Al-1	249.2	.0012303	669	7.0
Al-1	248.4	.0013093	1160	12.2
Al-1	248.3	.0013141	1163	12.2
Al-1	248.3	.0012111	1172	12.3
Al-1	248.4	.0011969	1177	12.4
Al-1	248.2	.0012429	1236	13.0
Al-1	248.2	.0011442	1237	13.0
Al-1	248.2	.0012298	1246	13.1
Al-1	248.2	.0012851	1251	13.1
Al-1	248.1	.0011092	1317	13.8
Al-1	248.0	.0012081	1324	13.9
Al-1	248.1	.0011092	1331	14.0
Al-1	248.0	.0012300	1335	14.0
Al-1	248.0	.0012521	1335	14.0
Al-1	248.0	.0012509	1349	14.2
Al-1	248.0	.0012974	1349	14.2
Al-1	247.9	.0012129	1421	14.9
Al-1	247.8	.0012978	1421	14.9
Al-1	247.8	.0012980	1439	15.1
Al-1	247.8	.0013103	1439	15.1
Al-1	247.6	.0012151	1516	15.9
Al-1	247.6	.0011758	1529	16.1
Al-1	247.6	.0012390	1533	16.1
Al-2	412.5	.0009685	200	2.2
Al-2	412.2	.0010852	208	2.2
Al-2	412.4	.0009689	209	2.2
Al-2	412.5	.0009626	213	2.2
Al-2	412.4	.0010525	216	2.3
Al-2	412.2	.0010565	226	2.4
Al-2	412.4	.0010496	227	2.4

62

TABLE 3.3 (Continued)

DAMPING OF ALUMINUM SPECIMENS WITH NODE WIRE ATTACHMENT

Specimen	Frequency rad/sec	Damping Ratio ζ	Strain 10^{-6}	Stress KSI
Al-2	412.4	.0010013	235	2.5
Al-2	412.2	.0010300	246	2.6
Al-2	412.4	.0011030	246	2.6
Al-2	412.5	.0010279	250	2.6
Al-2	412.3	.0011055	360	3.8
Al-2	412.4	.0010733	368	3.9
Al-2	411.9	.0011006	393	4.1
Al-2	412.2	.0011318	395	4.2
Al-2	412.4	.0010118	400	4.2
Al-2	412.0	.0010596	410	4.3
Al-2	411.9	.0011922	431	4.5
Al-2	412.2	.0011614	433	4.6
Al-2	412.3	.0010330	435	4.6
Al-2	412.0	.0010996	449	4.7
Al-2	411.8	.0012359	474	5.0
Al-2	411.9	.0010204	492	5.2
Al-3	2249	.0003404	16.5	.17
Al-3	2249	.0004235	17.5	.18
Al-3	2246	.0001802	18.9	.20
Al-3	2247	.0002103	20.2	.21
Al-3	2248	.0000988	20.8	.22
Al-3	2246	.0003704	20.9	.22
Al-3	2248	.0001742	22.1	.23
Al-3	2247	.0004038	23.9	.25
Al-3	2247	.0002429	26.4	.28
Al-3	2247	.0002188	27.7	.29
Al-3	2247	.0001996	29.8	.31
Al-3	2248	.0004310	47.6	.50
Al-3	2248	.0003921	48.6	.51
Al-3	2249	.0003920	51.3	.54
Al-3	2248	.0003504	52.3	.55
Al-3	2248	.0003976	53.8	.56
Al-3	2250	.0003850	54.9	.58
Al-3	2250	.0004083	55.3	.58
Al-3	2249	.0004038	57.9	.61
Al-3	2249	.0002446	58.7	.62
Al-3	2248	.0003949	59.5	.62
Al-3	2249	.0003373	59.9	.63

TABLE 3.4

SUMMARY OF ALUMINUM DAMPING RESULTS IN VALIDATION PROCEDURE

SPECIMEN	CENTER WIRES (MOHR'S RESULTS)	CENTER WIRES (CURRENT TESTS)	NODE WIRES (CURRENT TESTS)
Al-1	.00114	.00123	.00124
Al-2	.00105	.00107	.00106
Al-3	.000324	.000436	.000326

TABLE 3.5

MATERIAL DAMPING IN ALUMINUM SPECIMENS

Specimen	Frequency rad/sec	Damping Ratio ζ	Strain 10^{-6}	Stress KSI
Al-4	201.5	.0013330	748	7.9
Al-4	201.4	.0010496	786	8.3
Al-4	201.5	.0012644	807	8.5
Al-4	201.4	.0012506	813	8.5
Al-4	201.4	.0012720	820	8.6
Al-4	201.3	.0013179	857	9.0
Al-4	201.4	.0013318	861	9.0
Al-4	201.4	.0012444	862	9.0
Al-4	201.3	.0012590	897	9.4
Al-4	201.2	.0012302	902	9.5
Al-4	201.3	.0012080	907	9.5
Al-4	201.0	.0012182	1056	11.1
Al-4	200.9	.0013000	1101	11.6
Al-4	200.9	.0013018	1106	11.6
Al-4	200.8	.0012413	1110	11.7
Al-4	200.8	.0012641	1160	12.2
Al-4	200.8	.0013044	1166	12.2
Al-4	200.7	.0013012	1169	12.3
Al-4	200.7	.0012354	1201	12.6
Al-4	200.6	.0013000	1222	12.8
Al-4	200.6	.0012353	1227	12.9
Al-5	111.1	.0023742	812	8.5
Al-5	110.9	.0026207	891	9.4
Al-5	110.8	.0025151	910	9.6
Al-5	110.6	.0027838	951	10.0
Al-5	110.5	.0030827	953	10.0
Al-5	110.4	.0035275	1002	10.5
Al-5	110.4	.0030750	1012	10.6
Al-5	110.5	.0036301	1021	10.7
Al-5	110.2	.0037109	1044	11.0
Al-5	109.9	.0046911	1118	11.7
Al-5	110.0	.0046881	1138	11.9
Al-6	203.1	.0017529	762	8.0
Al-6	203.8	.0014728	811	8.5
Al-6	204.1	.0014586	825	8.7
Al-6	203.7	.0018114	829	8.7
Al-6	203.6	.0017429	835	8.8
Al-6	203.7	.0016393	844	8.9
Al-6	203.7	.0014547	863	9.1
Al-6	203.9	.0015092	870	9.1

65

TABLE 3.5 (Continued)

MATERIAL DAMPING IN ALUMINUM SPECIMENS

Specimen	Frequency rad/sec	Damping Ratio r	Strain 10^{-6}	Stress KSI
Al-6	204.0	.0016279	876	9.2
Al-6	203.6	.0016514	877	9.2
Al-6	203.5	.0018751	891	9.4
Al-6	203.5	.0018245	896	9.4
Al-6	203.5	.0017841	908	9.5
Al-6	203.8	.0016685	920	9.7
Al-6	203.8	.0015918	927	9.7
Al-6	203.8	.0016180	934	9.8
Al-6	203.4	.0019003	938	9.9
Al-6	203.4	.0018181	941	9.9
Al-6	203.4	.0018255	942	9.9
Al-6	203.3	.0019362	944	9.9
Al-6	203.8	.0018016	944	9.9
Al-6	203.4	.0019694	956	10.0
Al-6	203.2	.0020630	964	10.1
Al-6	203.3	.0020519	968	10.2
Al-6	203.2	.0020465	982	10.3
Al-6	203.6	.0017430	1016	10.7
Al-6	203.2	.0020985	1018	10.7
Al-6	203.2	.0019965	1022	10.7
Al-6	203.1	.0022239	1023	10.7
Al-6	203.0	.0022421	1028	10.8
Al-6	203.1	.0022816	1043	11.0
Al-6	203.4	.0018531	1092	11.5
Al-6	202.7	.0027940	1129	11.9
Al-6	202.6	.0028403	1136	11.9
Al-6	202.7	.0028035	1151	12.1
Al-6	203.1	.0021601	1182	12.4
Al-7	401.8	.0023094	127	1.3
Al-7	401.1	.0018953	133	1.4
Al-7	401.1	.0017787	137	1.4
Al-7	401.3	.0016206	137	1.4
Al-7	401.2	.0010469	140	1.5
Al-7	400.9	.0014825	146	1.5
Al-7	401.3	.0016050	147	1.5
Al-7	401.6	.0017002	154	1.6
Al-7	401.1	.0017389	154	1.6
Al-7	401.3	.0020965	155	1.6
Al-7	401.8	.0024713	155	1.6
Al-7	401.0	.0014023	156	1.6

TABLE 3.5 (Continued)

MATERIAL DAMPING IN ALUMINUM SPECIMENS

Specimen	Frequency rad/sec	Damping Ratio r	Strain 10^{-6}	Stress KSI
Al-7	401.2	.0017644	157	1.6
Al-7	401.3	.0015503	164	1.7
Al-7	400.8	.0015355	165	1.7
Al-7	401.7	.0013991	172	1.8
Al-7	401.2	.0018520	175	1.8
Al-7	401.0	.0014520	176	1.8
Al-7	401.4	.0014005	181	1.9
Al-7	400.9	.0011129	183	1.9
Al-7	401.2	.0022635	185	1.9
Al-7	401.8	.0022209	185	1.9
Al-7	401.6	.0013619	193	2.0
Al-7	401.6	.0017822	205	2.2
Al-7	401.5	.0017285	211	2.2
Al-7	401.2	.0011245	223	2.3
Al-7	401.5	.0012266	225	2.4
Al-7	401.6	.0017737	237	2.5
Al-7	401.5	.0018741	242	2.5
Al-7	401.3	.0015076	250	2.6
Al-7	401.4	.0012160	250	2.6
Al-7	401.4	.0015682	271	2.8
Al-7	401.2	.0016233	280	2.9
Al-7	401.4	.0015185	281	2.9
Al-7	401.3	.0022020	283	3.0
Al-7	401.6	.0021877	291	3.1
Al-7	401.3	.0019517	300	3.2
Al-7	401.2	.0016583	313	3.3
Al-7	401.3	.0021546	336	3.5
Al-7	401.5	.0020008	344	3.6
Al-7	401.4	.0019991	351	3.7
Al-7	401.2	.0017519	361	3.8
Al-7	401.4	.0019537	409	4.3
Al-7	401.2	.0016680	414	4.4
Al-8	629.8	.0015605	53.9	.57
Al-8	629.8	.0016412	56.0	.59
Al-8	629.1	.0016005	57.1	.60
Al-8	629.4	.0015679	59.7	.63
Al-8	629.6	.0013071	65.3	.69
Al-8	629.9	.0014613	68.6	.72
Al-8	629.1	.0016640	69.9	.73
Al-8	629.4	.0015567	72.3	.76

TABLE 3.5 (Continued)

MATERIAL DAMPING IN ALUMINUM SPECIMENS

Specimen	Frequency rad/sec	Damping Ratio ζ	Strain 10^{-6}	Stress KSI
Al-8	629.8	.0016558	78.7	.83
Al-8	629.4	.0015245	83.7	.88
Al-8	629.3	.0014057	84.9	.89
Al-8	629.1	.0014127	88.4	.93
Al-8	628.9	.0021124	133	1.4
Al-8	629.2	.0021001	135	1.4
Al-8	629.0	.0017491	143	1.5
Al-8	629.5	.0021136	145	1.5
Al-8	628.9	.0021307	173	1.8
Al-8	629.1	.0020656	175	1.8
Al-8	629.0	.0017661	178	1.9
Al-8	629.3	.0019459	189	2.0
Al-8	628.8	.0020045	225	2.4
Al-8	628.9	.0016661	226	2.4
Al-8	629.0	.0020501	228	2.4
Al-8	629.2	.0018178	241	2.5
Al-9	1124	.0010944	27.6	.29
Al-9	1124	.0013609	34.0	.36
Al-9	1124	.0012261	34.6	.36
Al-9	1125	.0013941	37.4	.39
Al-9	1124	.0010906	44.6	.47
Al-9	1124	.0010744	45.1	.47
Al-9	1124	.0013507	45.4	.48
Al-9	1126	.0011738	45.4	.48
Al-9	1124	.0011601	46.2	.49
Al-9	1124	.0010941	46.4	.49
Al-9	1124	.0010723	49.4	.52
Al-9	1125	.0011617	50.5	.53
Al-9	1124	.0011815	57.9	.61
Al-9	1126	.0011342	58.4	.61
Al-9	1124	.0009598	59.4	.62
Al-9	1124	.0012332	60.0	.63
Al-9	1124	.0012643	60.2	.63
Al-9	1125	.0012126	60.7	.64
Al-9	1124	.0011600	62.9	.66
Al-9	1124	.0011834	64.2	.67
Al-9	1126	.0011223	74.8	.79
Al-9	1124	.0012407	78.6	.83
Al-9	1124	.0011329	79.1	.83
Al-9	1124	.0011592	80.0	.84

TABLE 3.5 (Continued)

MATERIAL DAMPING IN ALUMINUM SPECIMENS

Specimen	Frequency rad/sec	Damping Ratio ζ	Strain 10^{-6}	Stress KSI
Al-9	1124	.0013650	82.4	.87
Al-9	1124	.0012566	84.0	.88
Al-9	1124	.0014108	84.1	.88
Al-9	1125	.0013116	102	1.07
Al-9	1125	.0014539	116.1	1.22

69

TABLE 3.6

MATERIAL DAMPING IN ALUMINUM AS MEASURED BY MALAN

Specimen	Frequency rad/sec	Damping Ratio ζ	Strain 10^{-6}	Stress KSI
Al-6	203.9	.00211	927	10.2
Al-6	203.7	.00213	983	10.8
Al-6	203.5	.00212	1048	11.5
Al-6	203.5	.00253	1086	11.9
Al-6	202.6	.00318	1087	14.4
Al-6	203.2	.00240	1116	12.2
Al-6	203.1	.00277	1168	12.7
Al-6	203.0	.00262	1203	13.1
Al-6	202.9	.00280	1260	13.7
Al-6	202.6	.00331	1292	14.1
Al-6	202.5	.00342	1375	14.9
Al-6	201.8	.00417	1467	15.8
Al-6	201.8	.00430	1535	16.6
Al-6	201.1	.00668	1603	17.2
Al-6	200.6	.00604	1704	18.2
Al-6	200.8	.00584	1766	18.9
Al-7	402.0	.00152	303	3.4
Al-7	402.0	.00160	353	3.9
Al-7	402.0	.00149	388	4.3
Al-7	402.0	.00158	425	4.7
Al-7	401.9	.00178	469	5.2
Al-7	401.8	.00195	571	6.4
Al-7	401.1	.00197	634	7.1
Al-7	401.1	.00216	720	8.0
Al-7	400.9	.00227	804	8.9
Al-7	400.6	.00248	930	10.3
Al-7	400.3	.00278	1032	11.4
Al-7	400.0	.00328	1105	12.2
Al-7	399.8	.00343	1464	13.4
Al-7	398.2	.00550	1475	16.1
Al-7	398.5	.00507	1557	17.0

TABLE 3.7

DAMPING IN $[0]_8$ GRAPHITE/EPOXY SPECIMENS OF SIMILAR DIMENSIONS

Specimen	Frequency rad/sec	Damping Ratio ζ	Strain 10^{-6}	Stress KSI
$[0]_8$-1	289.5	.0006746	469	7.61
$[0]_8$-1	289.5	.0006908	471	7.66
$[0]_8$-1	289.5	.0006581	477	7.74
$[0]_8$-1	289.5	.0006383	487	7.90
$[0]_8$-1	289.5	.0005192	488	7.93
$[0]_8$-1	289.5	.0006757	490	7.96
$[0]_8$-1	289.5	.0006699	496	8.06
$[0]_8$-1	289.4	.0005268	506	8.22
$[0]_8$-1	289.4	.0005706	506	8.22
$[0]_8$-1	289.4	.0006261	509	8.27
$[0]_8$-1	289.4	.0006855	515	8.37
$[0]_8$-1	289.4	.0005900	523	8.50
$[0]_8$-1	289.0	.0006022	694	11.27
$[0]_8$-1	288.9	.0006111	701	11.38
$[0]_8$-1	288.9	.0006287	711	11.54
$[0]_8$-1	288.9	.0005943	712	11.56
$[0]_8$-1	288.9	.0006136	719	11.67
$[0]_8$-1	288.9	.0005931	725	11.77
$[0]_8$-1	288.9	.0005981	737	11.96
$[0]_8$-1	288.9	.0006271	737	11.96
$[0]_8$-1	288.8	.0006927	749	12.17
$[0]_8$-1	288.8	.0006322	762	12.37
$[0]_8$-1	288.8	.0005868	763	12.40
$[0]_8$-2	284.3	.0005659	572	9.45
$[0]_8$-2	284.3	.0005722	583	9.64
$[0]_8$-2	284.3	.0006285	584	9.66
$[0]_8$-2	284.3	.0006387	588	9.72
$[0]_8$-2	284.3	.0005781	590	9.76
$[0]_8$-2	284.3	.0006023	602	9.95
$[0]_8$-2	284.3	.0006418	604	9.99
$[0]_8$-2	284.3	.0006101	609	10.06
$[0]_8$-2	284.2	.0005221	610	10.08
$[0]_8$-2	284.2	.0005606	623	10.30
$[0]_8$-2	284.2	.0005584	630	10.41
$[0]_8$-2	283.9	.0004566	748	12.37
$[0]_8$-2	283.9	.0004805	748	12.37
$[0]_8$-2	283.8	.0004095	764	12.63
$[0]_8$-2	283.8	.0004794	766	12.66
$[0]_8$-2	283.8	.0004582	768	12.70
$[0]_8$-2	283.8	.0004294	772	12.76

TABLE 3.7 (Continued)

DAMPING IN $[0]_8$ GRAPHITE/EPOXY SPECIMENS
OF SIMILAR DIMENSIONS

Specimen	Frequency rad/sec	Damping Ratio ζ	Strain 10^{-6}	Stress KSI
$[0]_8$-2	283.7	.0005931	783	12.95
$[0]_8$-2	283.8	.0004263	786	12.99
$[0]_8$-2	283.7	.0004693	787	13.01
$[0]_8$-2	283.7	.0004251	791	13.08
$[0]_8$-2	283.7	.0004167	805	13.31
$[0]_8$-2	283.6	.0004174	812	13.43
$[0]_8$-3	288.8	.0006402	463	7.38
$[0]_8$-3	288.8	.0005773	465	7.42
$[0]_8$-3	288.4	.0006513	476	7.60
$[0]_8$-3	288.8	.0006226	480	7.66
$[0]_8$-3	288.7	.0006775	480	7.66
$[0]_8$-3	288.8	.0005936	482	7.69
$[0]_8$-3	288.7	.0005910	497	7.93
$[0]_8$-3	288.7	.0006091	498	7.95
$[0]_8$-3	288.7	.0006904	500	7.98
$[0]_8$-3	288.3	.0006107	513	8.18
$[0]_8$-3	288.7	.0005900	514	8.19
$[0]_8$-3	287.9	.0006509	650	10.37
$[0]_8$-3	287.9	.0006406	670	10.69
$[0]_8$-3	287.9	.0006959	671	10.70
$[0]_8$-3	287.8	.0006649	675	10.77
$[0]_8$-3	287.7	.0006829	682	10.88
$[0]_8$-3	287.7	.0005809	694	11.06
$[0]_8$-3	287.7	.0007025	696	11.11
$[0]_8$-3	287.8	.0007065	698	11.14
$[0]_8$-3	287.8	.0007397	710	11.32
$[0]_8$-3	287.6	.0006286	722	11.51
$[0]_8$-3	287.7	.0006561	726	11.59
$[0]_8$-3	287.7	.0005572	738	11.77
$[0]_8$-4	301.5	.0007554	504	8.34
$[0]_6$-4	301.5	.0004765	510	8.42
$[0]_8$-4	301.5	.0004794	516	8.53
$[0]_8$-4	301.4	.0004072	526	8.70
$[0]_8$-4	301.4	.0005409	528	8.73
$[0]_8$-4	301.4	.0006642	528	8.73
$[0]_8$-4	301.5	.0004766	532	8.79
$[0]_8$-4	301.4	.0004315	539	8.90
$[0]_8$-4	301.4	.0005520	545	9.00
$[0]_6$-4	301.4	.0004859	549	9.08
$[0]_8$-4	301.3	.0005076	549	9.08

TABLE 3.7 (Continued)

DAMPING IN $[0]_8$ GRAPHITE/EPOXY SPECIMENS OF SIMILAR DIMENSIONS

Specimen	Frequency rad/sec	Damping Ratio ζ	Strain 10^{-6}	Stress KSI
$[0]_8$-4	301.3	.0005076	554	9.16
$[0]_8$-4	300.8	.0005849	732	12.09
$[0]_8$-4	300.8	.0005392	739	12.21
$[0]_8$-4	300.8	.0005009	750	12.40
$[0]_8$-4	300.8	.0005380	752	12.43
$[0]_8$-4	300.8	.0004080	754	12.47
$[0]_8$-4	300.8	.0005184	763	12.62
$[0]_8$-4	300.7	.0004214	774	12.79
$[0]_8$-4	300.7	.0004884	776	12.83
$[0]_8$-4	300.7	.0005373	788	13.02
$[0]_8$-4	300.6	.0003500	791	13.08
$[0]_8$-4	300.8	.0004590	771	12.75

TABLE 3.8

DAMPING IN [0]$_8$ GRAPHITE/EPOXY SPECIMENS OF DIFFERENT FREQUENCIES

Specimen	Frequency rad/sec	Damping Ratio ζ	Strain 10^{-6}	Stress KSI
[0]$_8$-4	301.5	.0007554	504	8.34
[0]$_8$-4	301.5	.0004765	510	8.42
[0]$_8$-4	301.5	.0004794	516	8.53
[0]$_8$-4	301.4	.0004072	526	8.70
[0]$_8$-4	301.4	.0005409	528	8.73
[0]$_8$-4	301.4	.0006642	528	8.73
[0]$_8$-4	301.5	.0004766	532	8.79
[0]$_8$-4	301.4	.0004315	539	8.90
[0]$_8$-4	301.4	.0005520	545	9.00
[0]$_8$-4	301.4	.0004859	549	9.08
[0]$_8$-4	301.3	.0006586	549	9.08
[0]$_8$-4	301.3	.0005076	554	9.16
[0]$_8$-4	300.8	.0005849	732	12.09
[0]$_8$-4	300.8	.0005392	739	12.21
[0]$_8$-4	300.8	.0005009	750	12.40
[0]$_8$-4	300.8	.0005380	752	12.43
[0]$_8$-4	300.8	.0004080	754	12.47
[0]$_8$-4	300.8	.0005184	763	12.62
[0]$_8$-4	300.8	.0004590	771	12.75
[0]$_8$-4	300.7	.0004214	774	12.79
[0]$_8$-4	300.7	.0004884	776	12.83
[0]$_8$-4	300.7	.0005373	788	13.02
[0]$_8$-4	300.6	.0003500	791	13.08
[0]$_8$-5	486.0	.0006693	96	1.57
[0]$_8$-5	486.0	.0006603	102	1.65
[0]$_8$-5	485.9	.0005696	104	1.68
[0]$_8$-5	486.1	.0006739	107	1.74
[0]$_8$-5	485.0	.0005622	108	1.75
[0]$_8$-5	486.0	.0005920	112	1.81
[0]$_8$-5	486.1	.0006234	113	1.84
[0]$_8$-5	486.0	.0006069	119	1.93
[0]$_8$-5	486.0	.0004088	120	1.94
[0]$_8$-5	485.7	.0006428	300	4.87
[0]$_8$-5	485.8	.0005891	313	5.09
[0]$_8$-5	485.8	.0005397	319	5.18
[0]$_8$-5	485.7	.0006047	319	5.18
[0]$_8$-5	485.7	.0005525	323	5.25
[0]$_8$-5	485.8	.0005290	331	5.38
[0]$_8$-5	485.7	.0006256	337	5.47
[0]$_8$-5	485.6	.0006859	339	5.51

TABLE 3.8 (Continued)

DAMPING IN $[0]_8$ GRAPHITE/EPOXY SPECIMENS
OF DIFFERENT FREQUENCIES

Specimen	Frequency rad/sec	Damping Ratio ζ	Strain 10^{-6}	Stress KSI
$[0]_8$-5	485.6	.0006827	343	5.57
$[0]_8$-5	485.7	.0006220	351	5.70
$[0]_8$-5	485.8	.0005503	357	5.80
$[0]_8$-5	485.7	.0006181	364	5.92
$[0]_8$-6	932.1	.0005031	160	2.55
$[0]_8$-6	931.7	.0005431	165	2.64
$[0]_8$-6	931.2	.0005381	167	2.67
$[0]_8$-6	932.0	.0004550	175	2.80
$[0]_8$-6	930.8	.0006058	175	2.80
$[0]_8$-6	931.0	.0004749	182	2.90
$[0]_8$-6	931.5	.0006479	186	2.97
$[0]_8$-6	931.6	.0004219	188	3.00
$[0]_8$-6	932.0	.0004223	190	3.03
$[0]_8$-6	931.6	.0005359	190	3.03
$[0]_8$-6	931.5	.0004001	192	3.06
$[0]_8$-6	930.8	.0005069	193	3.07
$[0]_8$-6	931.1	.0005960	200	3.19
$[0]_8$-6	931.6	.0004216	203	3.23
$[0]_8$-6	931.5	.0005670	205	3.23
$[0]_8$-6	931.3	.0003783	206	3.29
$[0]_8$-6	931.5	.0004565	207	3.31
$[0]_8$-6	931.6	.0004914	209	3.34
$[0]_8$-6	930.7	.0005875	216	3.45
$[0]_8$-6	931.3	.0004020	222	3.54
$[0]_8$-6	931.5	.0005200	228	3.64
$[0]_8$-6	931.1	.0003901	240	3.83
$[0]_8$-7	1492	.0005272	16.4	0.26
$[0]_8$-7	1490	.0007195	19.2	0.30
$[0]_8$-7	1492	.0004741	21.9	0.35
$[0]_8$-7	1492	.0006782	23.0	0.36
$[0]_8$-7	1492	.0004107	23.4	0.38
$[0]_8$-7	1491	.0005564	25.9	0.41
$[0]_8$-7	1493	.0005788	26.5	0.42
$[0]_8$-7	1492	.0004750	28.2	0.45
$[0]_8$-7	1492	.0005000	31.1	0.49
$[0]_8$-7	1491	.0004888	49.3	0.78
$[0]_8$-7	1491	.0004440	57.3	0.90
$[0]_8$-7	1492	.0004098	63.9	1.02
$[0]_8$-7	1491	.0007615	68.6	1.09
$[0]_8$-7	1492	.0003576	72.2	1.15

TABLE 3.8 (Continued)

DAMPING IN $[0]_8$ GRAPHITE/EPOXY SPECIMENS OF DIFFERENT FREQUENCIES

Specimen	Frequency rad/sec	Damping Ratio ζ	Strain 10^{-6}	Stress KSI
$[0]_8$-7	1492	.0004627	74.1	1.17
$[0]_8$-7	1492	.0005058	81.9	1.29
$[0]_8$-7	1491	.0005374	85.9	1.36
$[0]_8$-7	1492	.0004931	94.5	1.49

*Entries for specimen 4 are the same as those found in Table 3.5

TABLE 3.9

DAMPING IN $[90]_8$ GRAPHITE/EPOXY SPECIMENS AT DIFFERENT FREQUENCIES

Specimen	Frequency rad/sec	Damping Ratio ζ	Strain 10^{-6}	Stress MPA
$[90]_8-1$	267.1	.0053468	250	0.32
$[90]_8-1$	266.9	.0050876	270	0.34
$[90]_8-1$	267.0	.0053947	272	0.35
$[90]_8-1$	267.1	.0055529	281	0.36
$[90]_8-1$	267.1	.0057677	337	0.43
$[90]_8-1$	267.1	.0053905	338	0.43
$[90]_8-1$	267.2	.0052550	345	0.44
$[90]_8-1$	267.2	.0057623	346	0.44
$[90]_8-1$	267.0	.0051192	351	0.45
$[90]_8-1$	267.0	.0054131	364	0.46
$[90]_8-1$	267.0	.0055037	379	0.48
$[90]_8-1$	267.1	.0054688	385	0.49
$[90]_8-1$	267.0	.0054883	454	0.58
$[90]_9-1$	266.9	.0056325	457	0.58
$[90]_8-1$	267.1	.0056554	462	0.59
$[90]_8-1$	266.8	.0057862	465	0.59
$[90]_8-1$	266.9	.0053833	469	0.60
$[90]_8-1$	266.9	.0052813	487	0.62
$[90]_8-1$	267.0	.0052863	512	0.65
$[90]_8-1$	266.9	.0055454	512	0.65
$[90]_8-1$	266.9	.0057574	615	0.78
$[90]_8-1$	267.2	.0055679	617	0.78
$[90]_8-1$	267.0	.0054131	627	0.80
$[90]_8-1$	267.0	.0056052	676	0.86
$[90]_8-2$	466.0	.0057347	42.6	0.06
$[90]_8-2$	465.4	.0059775	43.8	0.06
$[90]_8-2$	466.0	.0054839	44.6	0.06
$[90]_8-2$	465.8	.0055738	50.4	0.07
$[90]_8-2$	466.4	.0054561	73.3	0.09
$[90]_8-2$	465.9	.0058398	75.6	0.10
$[90]_8-2$	465.5	.0063127	76.6	0.10
$[90]_8-2$	465.9	.0068251	76.9	0.10
$[90]_8-2$	465.8	.0058512	84.6	0.11
$[90]_8-2$	465.3	.0069536	87.3	0.11
$[90]_8-2$	466.4	.0065889	104	0.13
$[90]_8-2$	466.3	.0055976	125	0.16
$[90]_8-2$	466.3	.0057851	125	0.16
$[90]_8-2$	465.9	.0059192	131	0.17
$[90]_8-2$	465.6	.0057376	135	0.17
$[90]_8-2$	465.7	.0062473	136	0.18

TABLE 3.9 (Continued)

DAMPING IN [90]$_8$ GRAPHITE/EPOXY SPECIMENS AT DIFFERENT FREQUENCIES

Specimen	Frequency rad/sec	Damping Ratio ζ	Strain 10^{-6}	Stress MPA
[90]$_8$-2	465.8	.0058262	145	0.19
[90]$_8$-2	466.0	.0060157	159	0.21
[90]$_8$-2	466.2	.0062432	187	0.24
[90]$_8$-2	466.4	.0060565	213	0.28
[90]$_8$-2	466.7	.0060985	215	0.28
[90]$_8$-3	900.7	.0069376	6.6	0.01
[90]$_8$-3	899.7	.0068057	16.3	0.02
[90]$_8$-3	900.3	.0063978	19.5	0.03
[90]$_8$-3	900.2	.0062527	20.7	0.03
[90]$_8$-3	900.0	.0062194	20.9	0.03
[90]$_8$-3	900.3	.0064791	23.3	0.03
[90]$_8$-3	898.3	.0062643	23.5	0.03
[90]$_8$-3	899.8	.0067832	56.9	0.08
[90]$_8$-3	900.5	.0064307	59.6	0.08
[90]$_8$-3	900.2	.0062633	65.3	0.09
[90]$_8$-3	900.3	.0074783	65.7	0.09
[90]$_8$-3	899.6	.0063316	69.9	0.09
[90]$_8$-3	897.8	.0060260	71.0	0.09
[90]$_8$-3	899.9	.0066946	190	0.25
[90]$_8$-3	899.4	.0074402	194	0.26
[90]$_8$-3	899.9	.0068847	207	0.27
[90]$_8$-3	899.8	.0069451	208	0.27

TABLE 3.10

DAMPING IN $[\pm 45]_{2s}$ GRAPHITE/EPOXY AS REPORTED BY MOHR [2]

Specimen	Frequency rad/sec	Damping Ratio ζ	Stress KSI
$[\pm 45]_{2s}-1$	17.95	0.56106	6.33
		0.56141	5.75
		0.52858	5.39
		0.50938	5.00
		0.53829	4.94
		0.53370	4.66
		0.57932	4.24
		0.52164	4.24
$[\pm 45]_{2s}-2$	29.62	0.54658	6.02
		0.54771	5.25
		0.56623	4.50
		0.53853	3.87
		0.54985	3.61
		0.58294	3.35
		0.54304	2.94
		0.54768	2.73
		0.55437	2.07
$[\pm 45]_{2s}-3$	54.16	0.61403	5.03
		0.59543	3.25
		0.65245	2.41
		0.59023	1.82
		0.65308	1.11
		0.57386	1.08
		0.57014	1.04
		0.57035	0.60
		0.55876	0.34
$[\pm 45]_{2s}-4$	171.04	0.66985	1.547
		0.66675	0.959
		0.66152	0.633
		0.65074	0.555
		0.66334	0.393
		0.65958	0.260
		0.64098	0.239
		0.65802	0.160
		0.65043	0.106

79

TABLE 3.11

DAMPING IN METAL MATRIX SPECIMENS

Specimen	Frequency rad/sec	Damping Ratio ζ	Strain 10^{-6}
P100/AZ91C/Ti	3105	.0003922	16.2
"	3105	.0004864	18.9
"	3106	.0003400	27.2
"	3103	.0003715	29.0
"	3106	.0002981	30.4
"	3106	.0003081	30.9
"	3105	.0003472	32.2
"	3103	.0003956	32.7
"	3106	.0003268	33.8
"	3106	.0004557	34.2
"	3105	.0004371	36.0
"	3103	.0002876	36.5
"	3106	.0003329	36.9
"	3106	.0003564	37.3
"	3102	.0004365	41.3
"	3105	.0004969	41.4
"	3106	.0003689	41.5
"	3101	.0003817	47.0
P55/AZ91C/Ti	2522	.0003951	36.9
"	2522	.0004798	41.2
"	2522	.0004060	42.6
"	2523	.0003463	43.8
"	2523	.0004010	45.9
"	2522	.0004243	45.9
"	2523	.0002936	46.6
"	2522	.0004712	47.5
"	2523	.0003196	47.5
"	2522	.0002406	49.4
"	2522	.0004589	50.8
"	2524	.0004058	51.1
"	2522	.0004049	51.4
"	2522	.0003764	53.0
"	2522	.0003479	55.4
"	2522	.0004131	58.7
"	2522	.0004416	60.1
P100/AZ91C/Mg	864.5	.0007114	36.0
"	864.9	.0011479	42.9
"	866.1	.0007313	52.5
"	864.7	.0013566	55.5

TABLE 3.11 (Continued)

DAMPING IN METAL MATRIX SPECIMENS
OF SIMILAR DIMENSIONS

Specimen	Frequency rad/sec	Damping Ratio ζ	Strain 10^{-6}
P100/AZ91C/Mg	864.6	.0004546	57.7
"	866.0	.0007374	59.5
"	865.4	.0005412	62.7
"	865.4	.0005043	63.1
"	866.0	.0007726	67.6
"	865.5	.0011916	67.7
"	865.3	.0006603	70.4
"	865.5	.0007063	71.0
"	865.4	.0006131	79.3
"	865.6	.0005553	82.1
"	865.2	.0012930	84.8
"	865.4	.0008314	86.5
"	865.2	.0009203	89.9
"	865.4	.0007139	92.5
"	865.5	.0010888	94.7
"	864.6	.0012904	98.1
"	865.4	.0010172	102.3
"	865.1	.0009475	106.4
"	865.4	.0010872	107.0
"	865.3	.0012739	108.5
"	865.3	.0012971	108.8
"	864.9	.0012565	111.5
"	865.0	.0010617	113.2
"	865.3	.0009967	115.1
"	865.4	.0012724	117.0
"	865.5	.0007652	119.2
"	864.7	.0006888	119.4
"	864.7	.0011913	121.7
"	865.4	.0010676	124.1
"	865.1	.0010801	130.0
"	865.2	.0010760	132.5
"	865.3	.0008469	132.5
"	865.3	.0011036	134.1
"	865.3	.0009552	134.7
"	865.0	.0010482	135.4
"	865.5	.0010371	137.8
"	865.1	.0011503	137.9
"	865.4	.0012328	145.6

TABLE 3.11 (Continued)

DAMPING IN METAL MATRIX SPECIMENS

Specimen	Frequency rad/sec	Damping Ratio ζ	Strain 10^{-6}
P100/AZ91C/Mg	864.8	.0012102	151.1
"	865.3	.0007924	152.2
"	865.4	.0010207	158.0
"	865.4	.0011128	161.4
"	865.3	.0011930	161.8
"	864.7	.0011327	162.5
"	865.1	.0010898	162.8
"	864.8	.0007412	164.9
"	865.7	.0012266	167.9
"	865.3	.0007903	175.7

TABLE 4.1

COMPOSITE DAMPING OF SIMILAR SPECIMENS OF $[0]_8$

SPECIMEN	FREQUENCY Hz	DAMPING RATIO (10^{-3})	STD DEVIATION (10^{-3})
1	46.0	0.622	0.048
2	45.2	0.512	0.082
3	45.9	0.642	0.047
4	47.8	0.514	0.090

TABLE 4.2

DAMPING RATIO OF MATRIX MATERIAL AS CALCULATED FROM DAMPING OF SPECIMENS OF SIMILAR GEOMETRY

SPECIMEN	RULE OF MIXTURES	COMPLEX MODULI	COMPLEX MODULI + SHEAR
1	.00104	0.0389	0.0384
2	.00085	0.0326	0.0322
3	.00107	0.0394	0.0389
4	.00086	0.0327	0.0322
AVERAGE FOR SPECIMENS OF SIMILAR GEOMETRY	.00096	0.0359	0.0354

TABLE 4.3

DAMPING RATIO OF MATRIX MATERIAL AS CALCULATED
FROM DAMPING OF $[0]_8$ SPECIMENS OF DIFFERENT FREQUENCIES

SPECIMEN	RULE OF MIXTURES	COMPLEX MODULI	COMPLEX MODULI + SHEAR
4	.00086	0.0327	0.0322
5	.00100	0.0375	0.0367
6	.00082	0.0303	0.0291
7	.00087	0.0317	0.0297
AVERAGE	.00089	0.0331	0.0319
REFERENCE AVERAGE FOR SPECIMENS OF SIMILAR GEOMETRY (FROM TABLE 4.2)	.00096	0.0359	0.0354

TABLE 4.4

DAMPING RATIO OF MATRIX MATERIAL AS CALCULATED
FROM DAMPING OF $[90]_8$ SPECIMENS OF DIFFERENT FREQUENCIES

SPECIMEN	RULE OF MIXTURES	COMPLEX MODULI	COMPLEX MODULI + SHEAR
1	.00913	0.0268	0.0268
2	.01001	0.0298	0.0298
3	.01103	0.0336	0.0336
AVERAGE	.01006	0.0301	0.0301
REFERENCE AVERAGE FOR SPECIMENS OF SIMILAR GEOMETRY (FROM TABLE 4.2)	.00096	0.0359	0.0354

TABLE 4.5

DYNAMIC YOUNG'S MODULUS FOR GRAPHITE/EPOXY

SPECIMEN	VALUE DERIVED FROM IN PLANE EXTENSIONAL TESTS (GPA)	VALUE FROM FLEXURAL TESTS (GPA)	TURNER VALUE (GPA)
$[0]_8-1$	130.0	112	98
$[0]_8-2$	130.0	114	98
$[0]_8-3$	130.0	110	98
$[0]_8-4$	130.0	114	98
$[0]_8-5$	130.0	112	98
$[0]_8-6$	130.0	110	98
$[0]_8-7$	130.0	109	98
$[90]_8-1$	10.5	8.8	7.9
$[90]_8-2$	10.5	8.9	7.9
$[90]_8-3$	10.5	9.1	7.9

TABLE 4.6

DAMPING OF P100/AZ91C/Mg METAL MATRIX SPECIMEN

THEORY	THEORETICAL VALUE	% DIFFERENCE FROM EXPERIMENTAL VALUE
RULE OF MIXTURES	.00089	-10.1
COMPLEX MODULI	.00273	175.8
COMPLEX MODULI + SHEAR	.00273	175.8
ZENER	.00105	6.1
EXPERIMENTAL AVERAGE	.00099	0.0

86
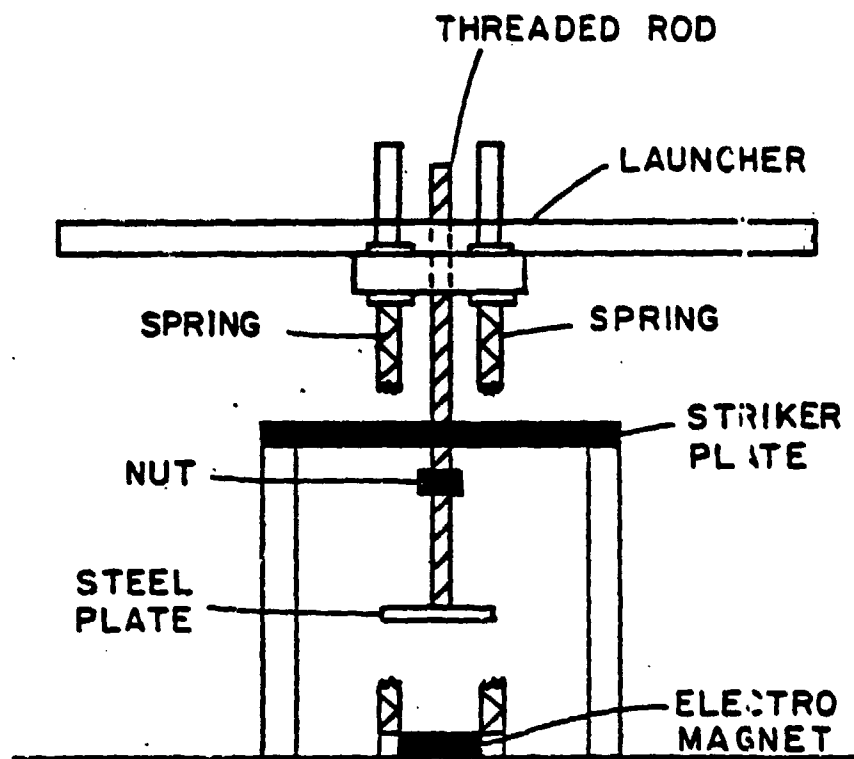
Figure 2.1   Tuned Excitation & Launch
Mechanism, (TELM) as used by Mohr
Prior to Modification

(C) FLIGHT

(B) RELEASE

(A) LAUNCHER IN COCKED POSITION
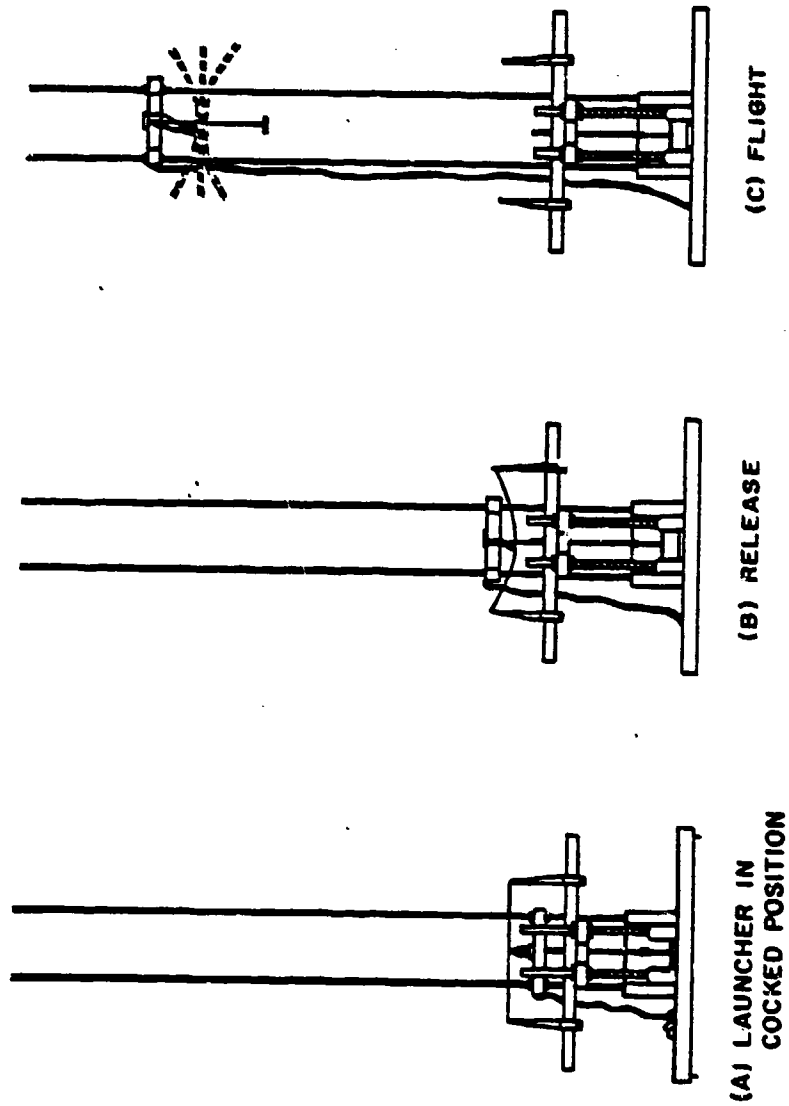
Figure 2.2   TELM Launch Sequence
Prior to Modification

88
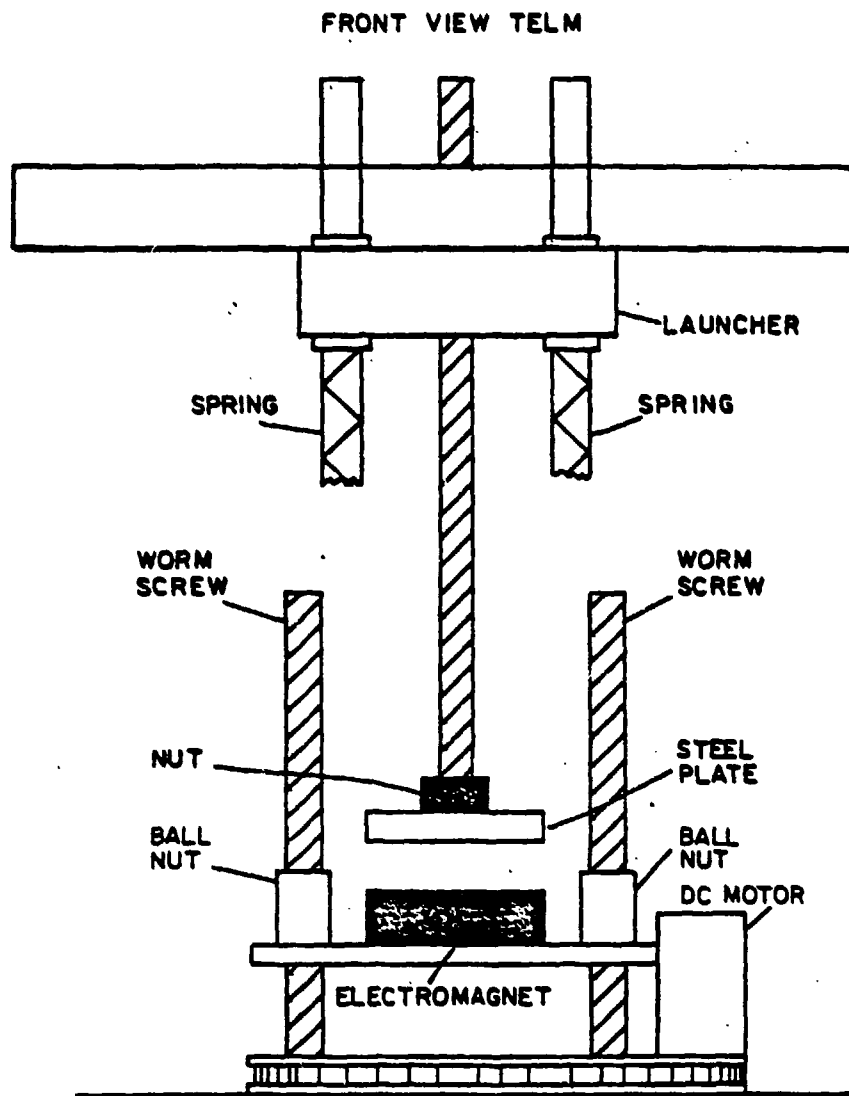
Figure 2.3   TELM Automated Cocking
Mechanism

89

SIDE VIEW TELM
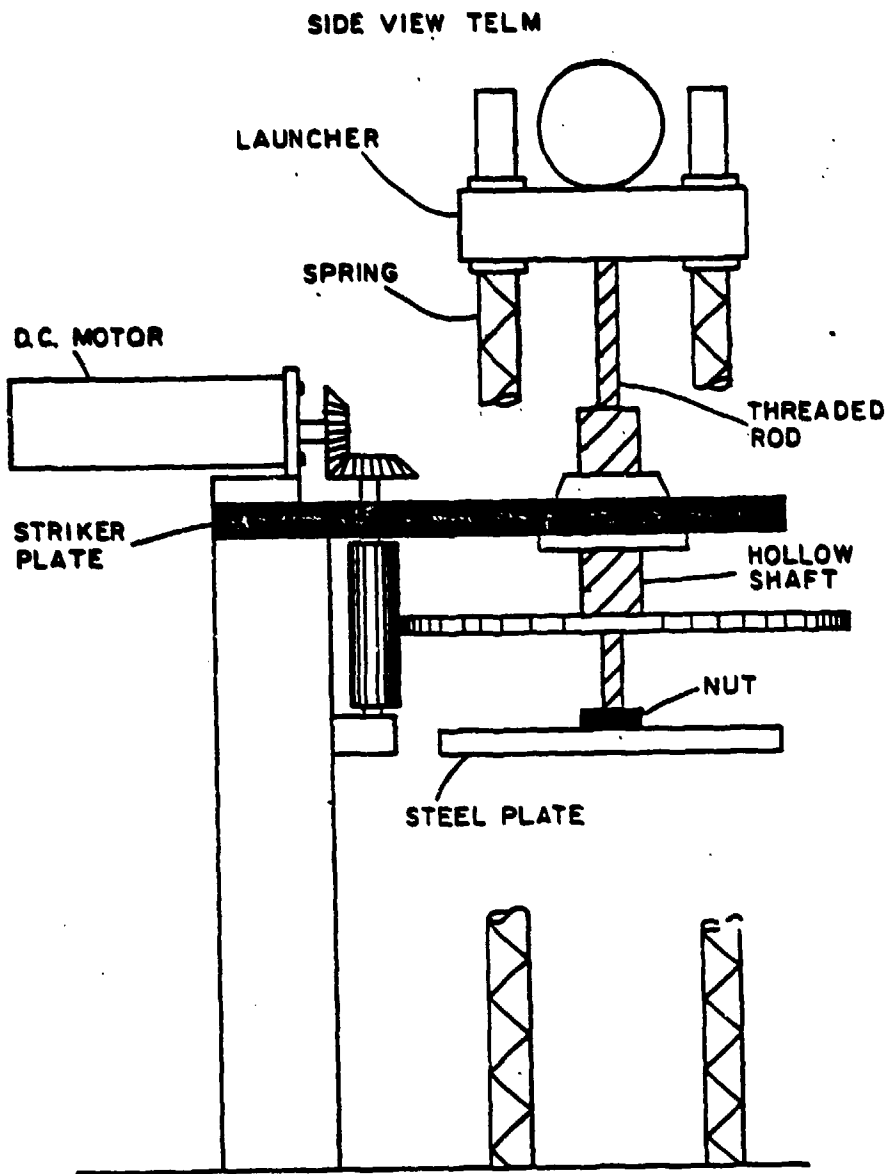

Figure 2.4   TELM Automated Stroke
   Adjustment

90
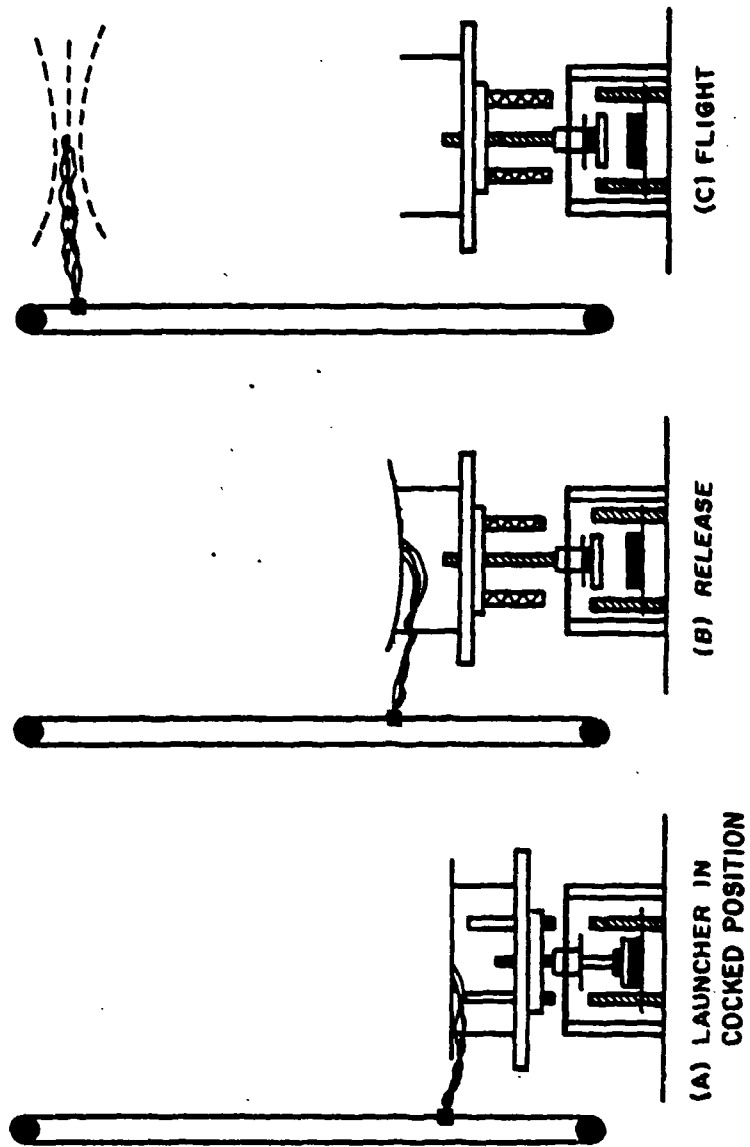
Figure 2.5   Current TELM Launch
Sequence

91
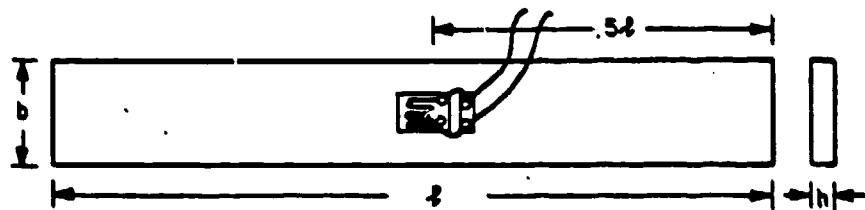
SPECIMEN WITH STRAIN GAUGE WIRES
MOUNTED AT THE CENTER
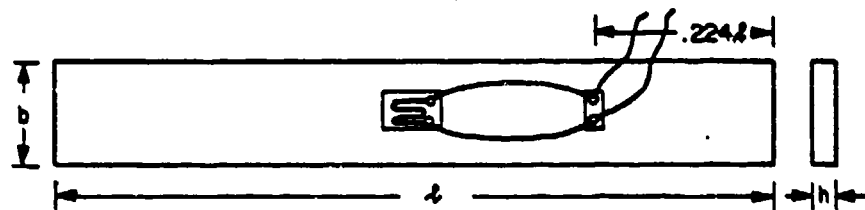
SPECIMEN WITH STRAIN GAUGE WIRES
MOUNTED AT THE NODE OF FIRST
FREE-FREE MODE

Figure 2.6   Specimen Configuration
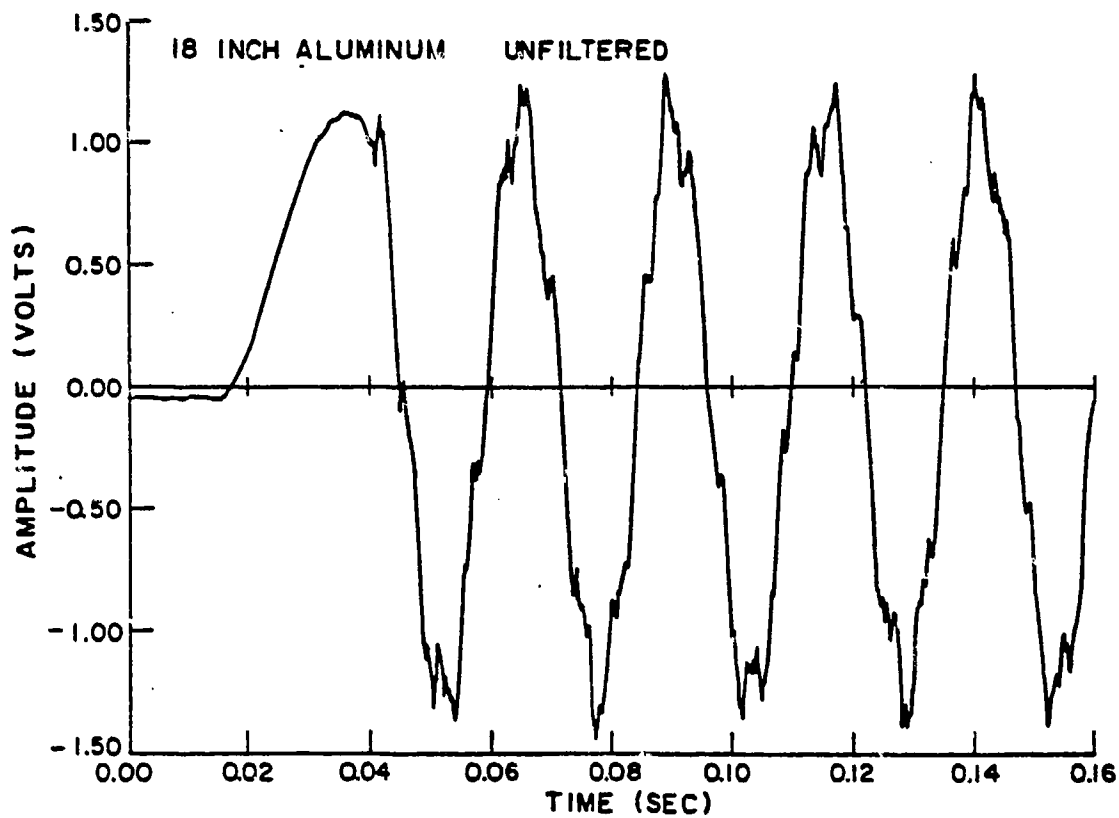
Figure 2.7 Unfiltered Strain Data vs. Time

93
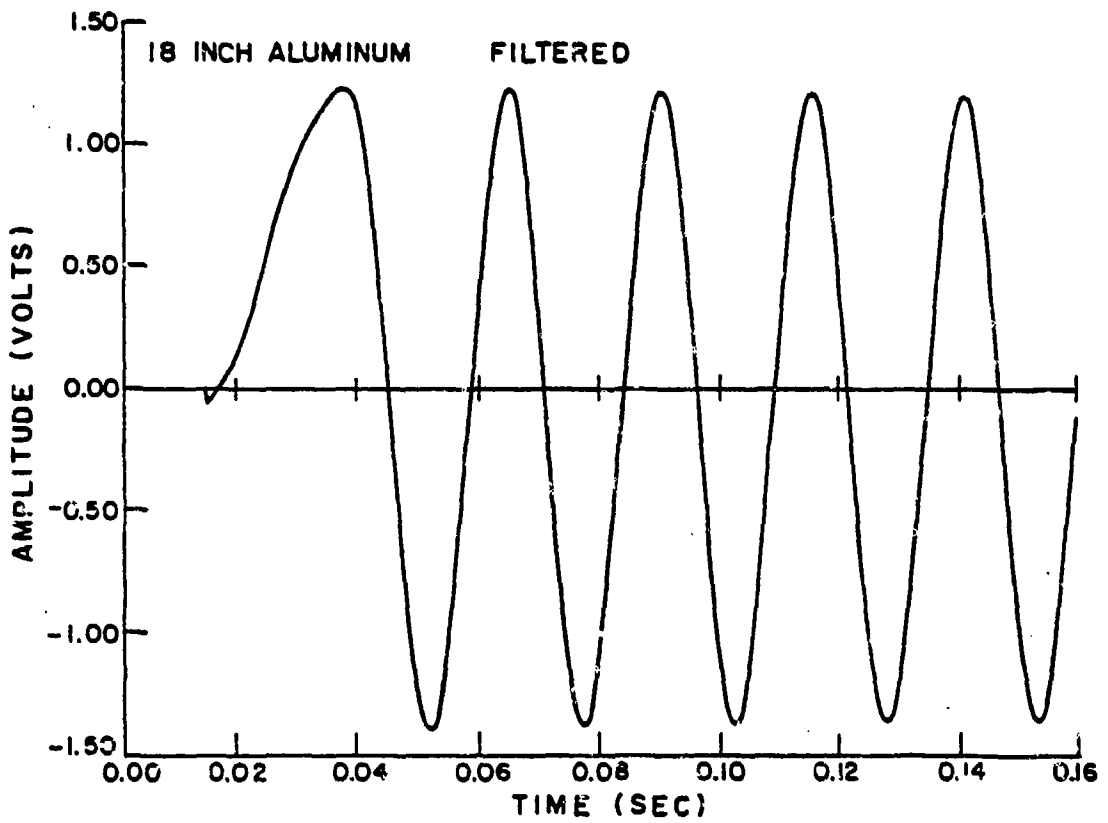
Figure 2.8 Filtered Strain Data vs. Time

94
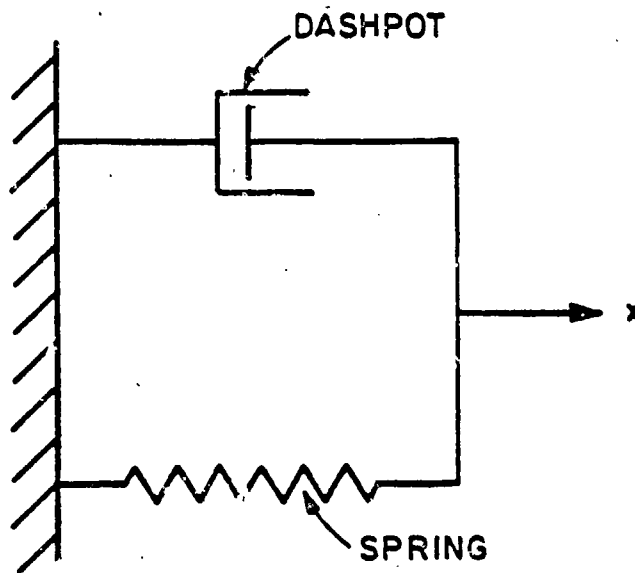
Figure 4.1 Conceptual Damping Model
of a Voight Solid
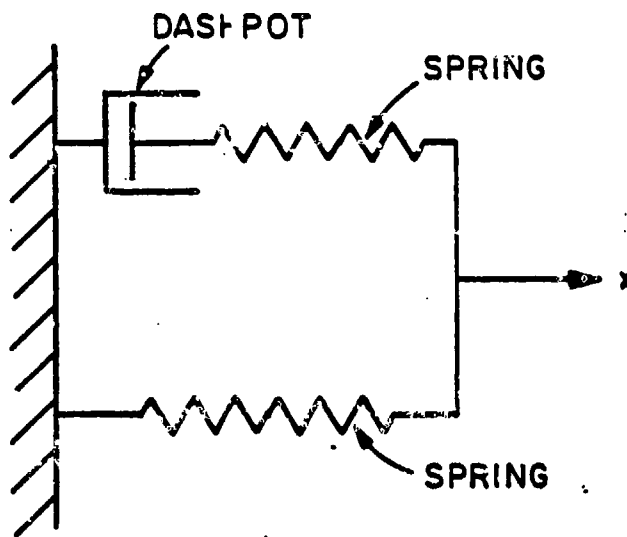
Figure 4.2 Conceptual Damping Model
of a Standard Linear Solid

95
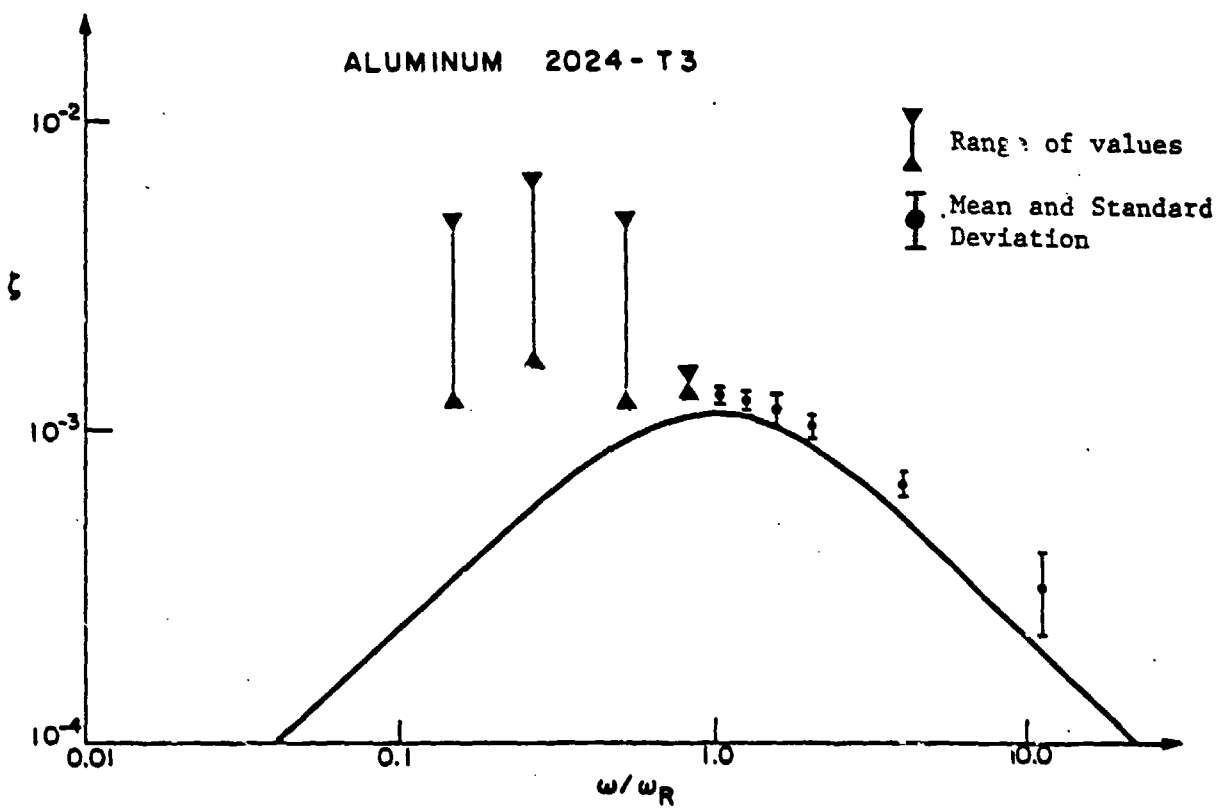
Figure 4.3   Damping Ratio vs. Frequency for Aluminum

96

DAMPING RATIO VS. STRESS FOR SPECIMENS WITH FIRST
FREE-FREE FREQUENCY BELOW ZENER RELAXTION
FREQUENCY
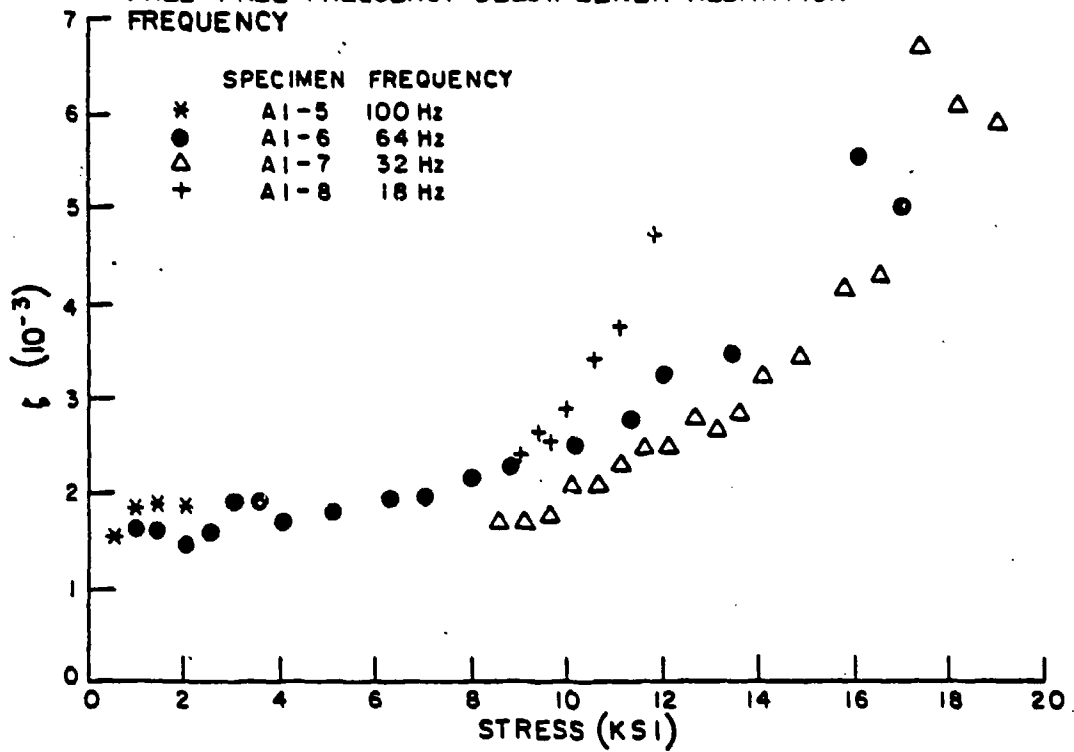
Figure 4.4   Damping Ratio vs. Stress Level for
Aluminum

97
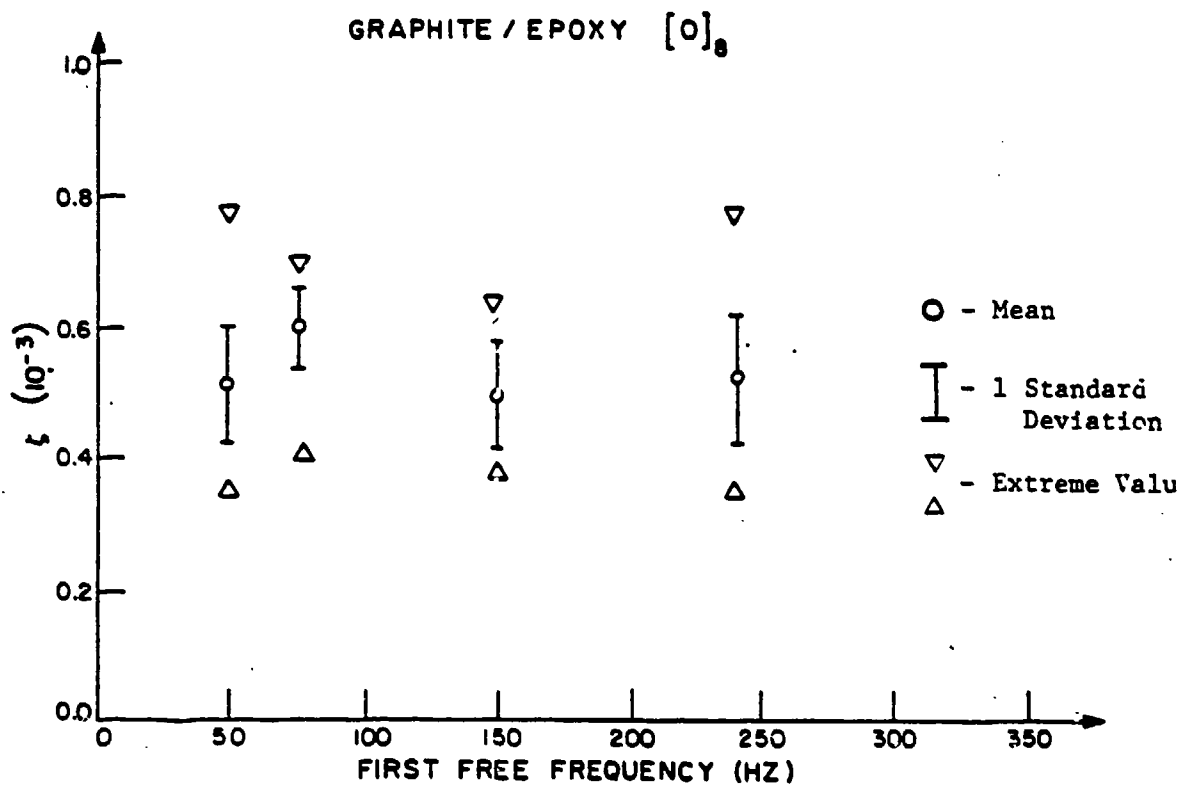
GRAPHITE / EPOXY $[0]_8$

Figure 4.5 Damping Ratio vs. Frequency for $[0]_8$
Graphite/Epoxy

98
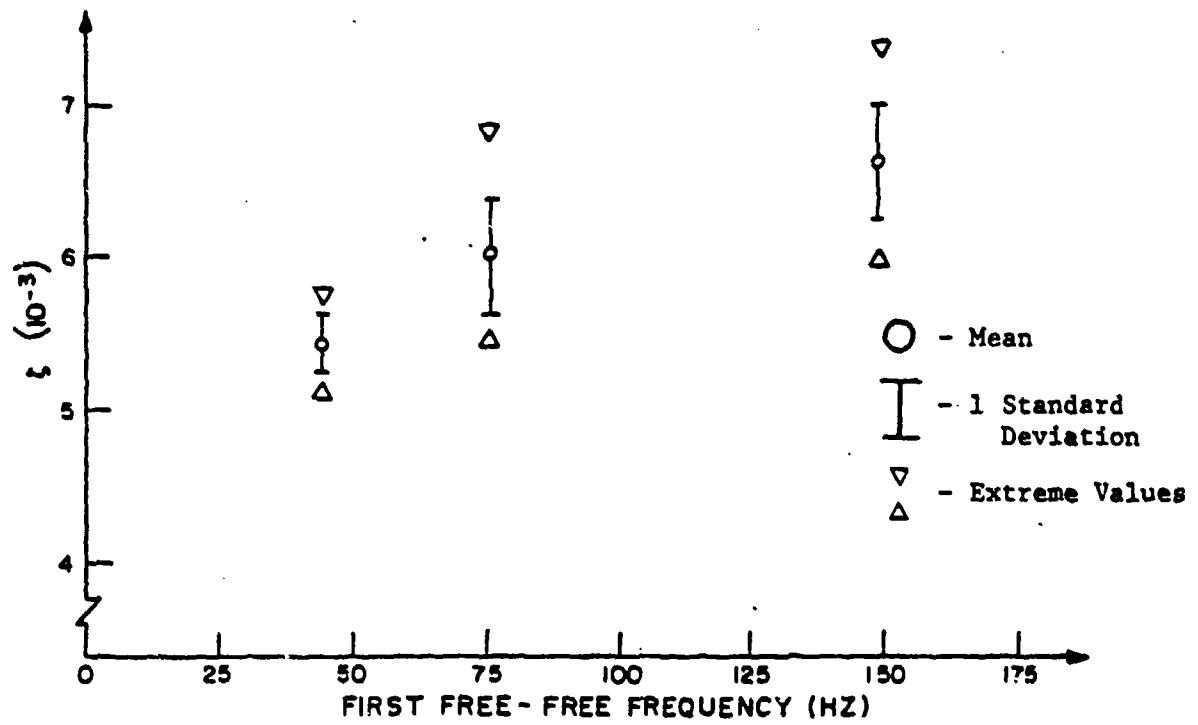
GRAPHITE / EPOXY $[90]_8$

Figure 4.6   Damping Ratio vs. Frequency for
$[90]_8$ Graphite/Epoxy

99
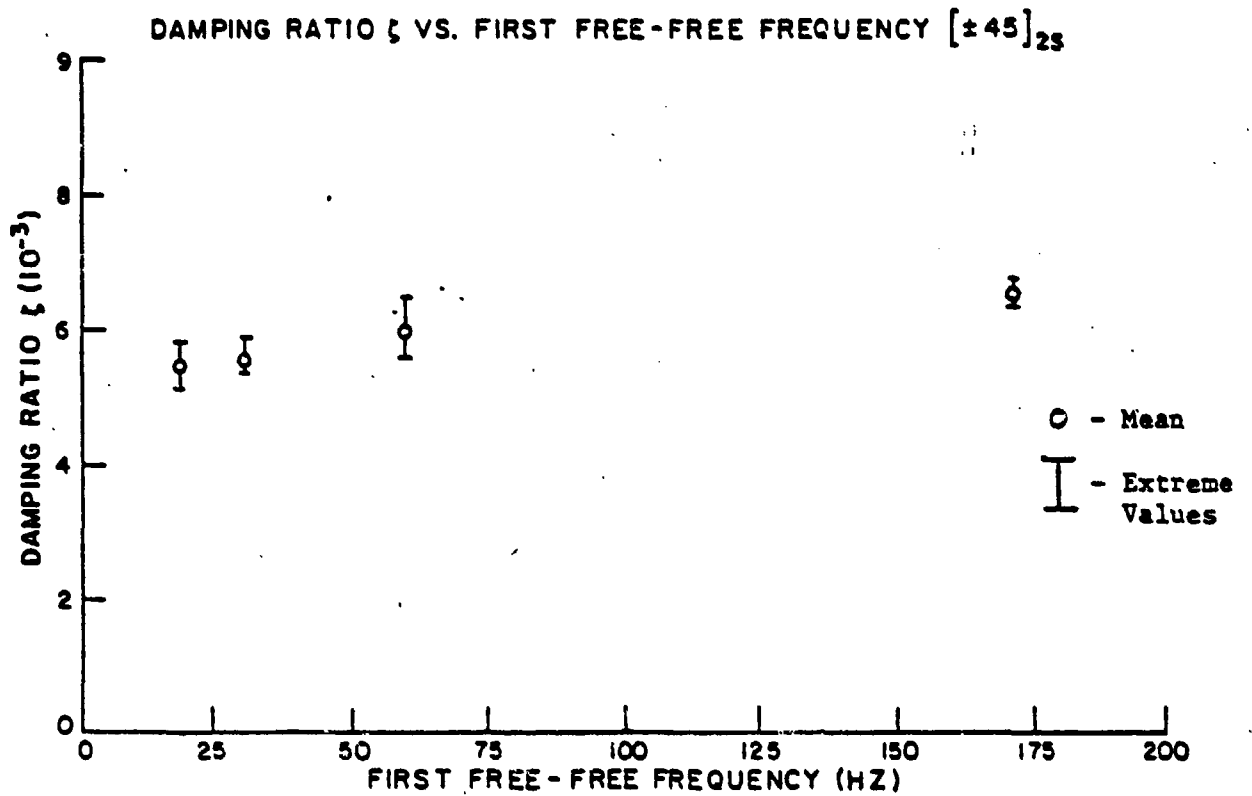
Figure 4.7 Damping Ratio vs. Frequency for $[\pm 45]_{2s}$
Graphite/Epoxy

100

DAMPING RATIO VS. FIBER ORIENTATION
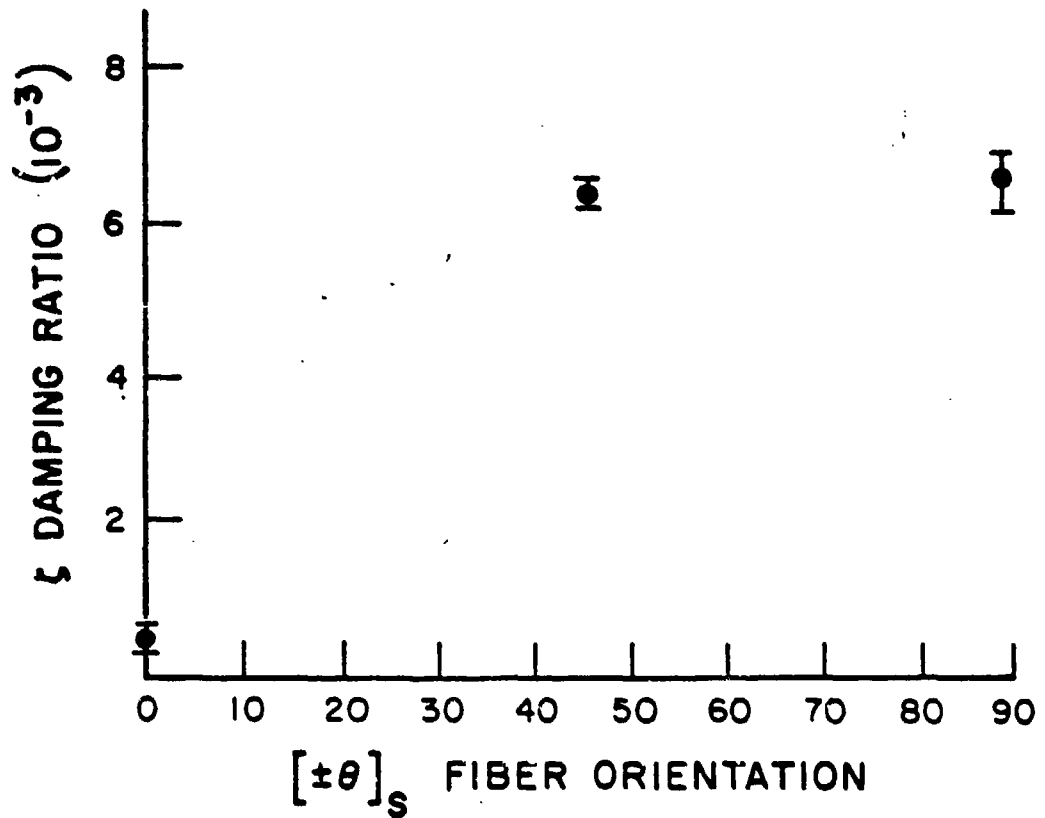
Figure 4.8 Damping Ratio vs. Fiber Orientation
for Graphite/Epoxy Specimens in the Frequency
Range 140Hz to 170Hz

101

Specimen	ω/ω_R
P100/AZ91C/Ti	10.2
P55/AZ91C/Ti	9.3
P100/AZ91C/Mg	.9

Zener Curve for Mg AZ91C

O — Mean

I — 1 Standard Deviation

▽ — Extreme Values
△
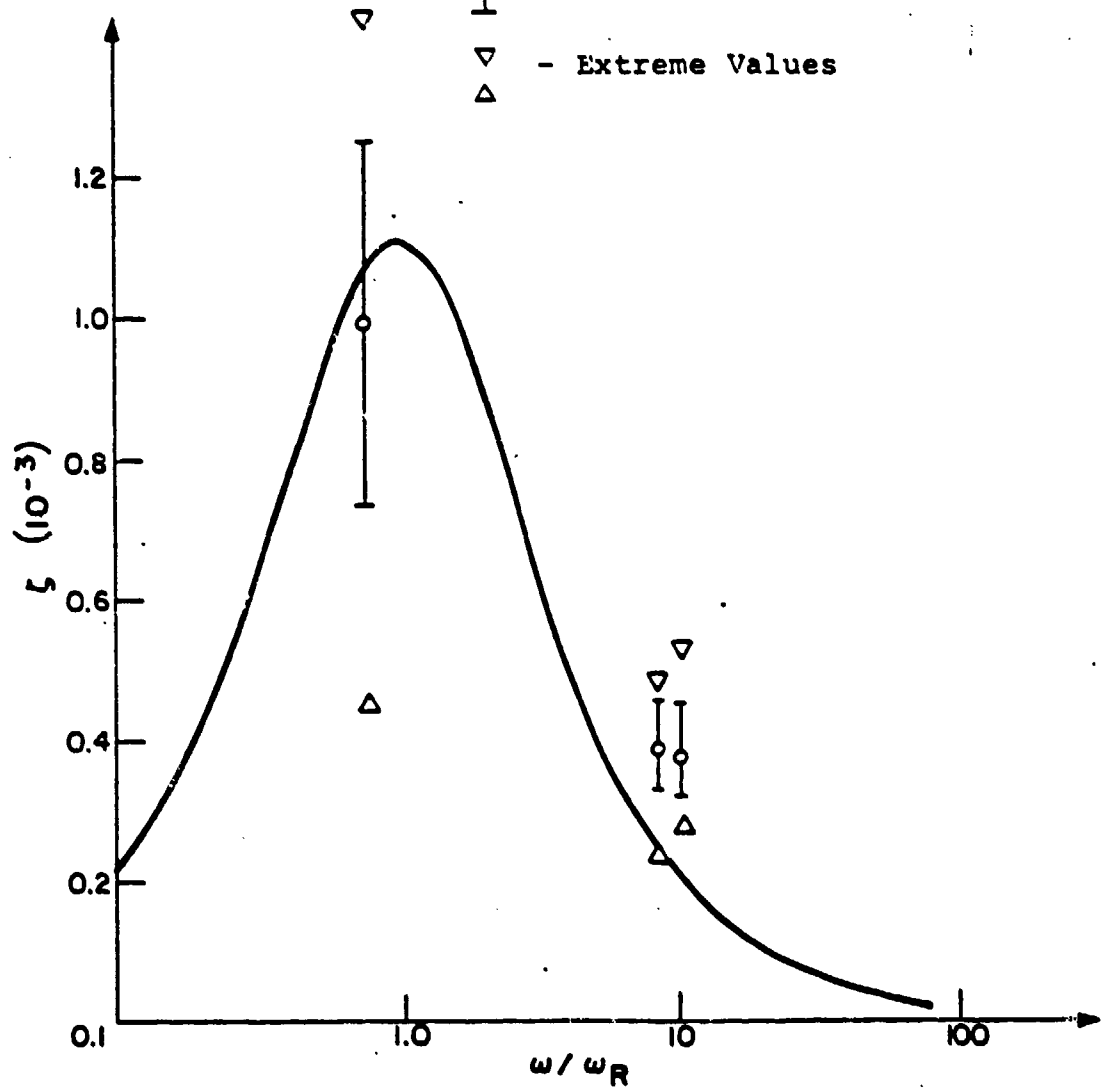
Figure 4.9 Damping of Metal Matrix Specimens vs. Frequency

102

APPENDIX A

MICROCOMPUTER PROGRAM

A flow chart of the microcomputer program and the interrupt handler, along with the actual assembly language listing are in this Appendix. The interrupt handler was run at 200Hz.

```
        ┌──────────────┐
        │    BEGIN     │
        └──────┬───────┘
               ↓
        ┌──────────────┐
        │  INITIALIZE  │
        │  CONSTANTS   │
        └──────┬───────┘
               ↓
    ┌──────────────────────┐
    │ INITIALIZE INTERRUPT │
    │     VECTOR TABLE     │
    └──────────┬───────────┘
               ↓
    ┌──────────────────────┐
    │  ENABLE INTERRUPTS    │
    └──────────┬───────────┘
               ↓
              ( )
               ↓
    ┌──────────────────────┐
    │   CONTINUOUS LOOP     │
    └──────────┬───────────┘
               ↓

        ┌──────────────┐
        │     END      │
        └──────────────┘
```
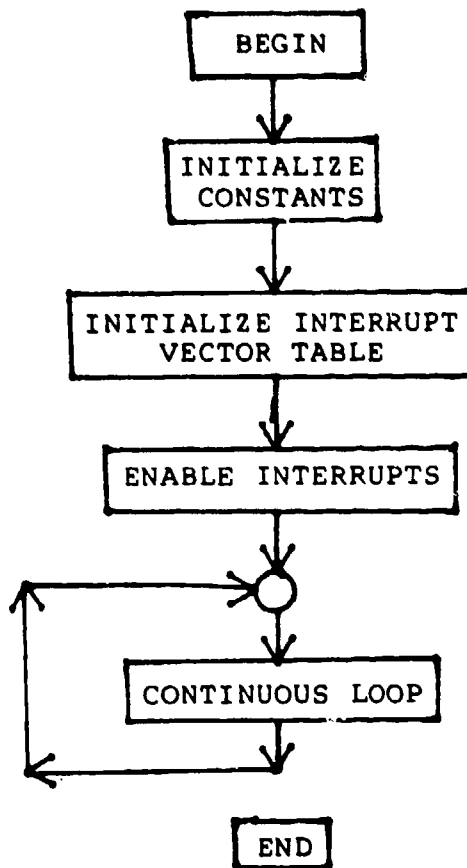
Figure A.1   Program Flow Chart
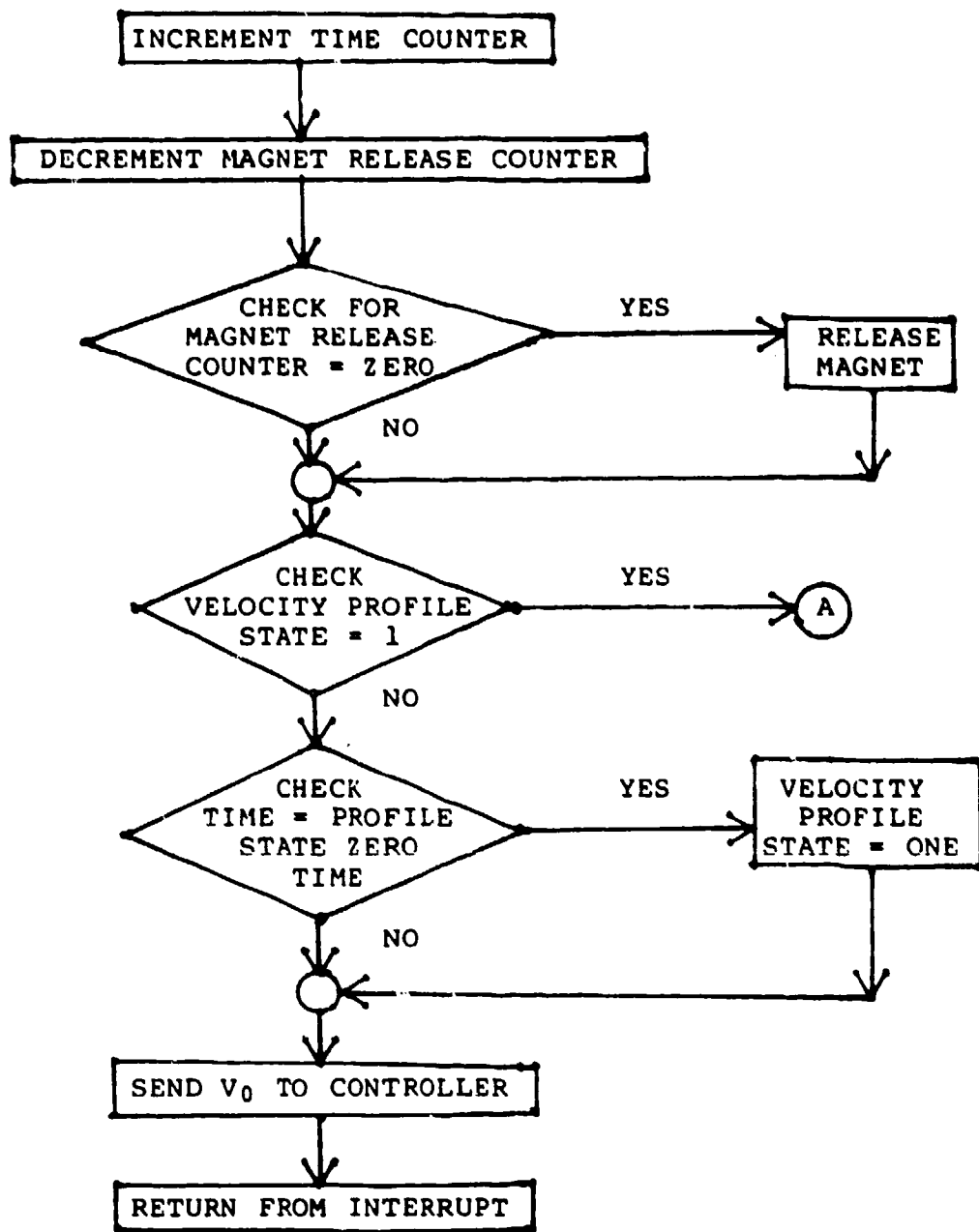
Figure A.2 Interrupt Handler Flow Chart

104
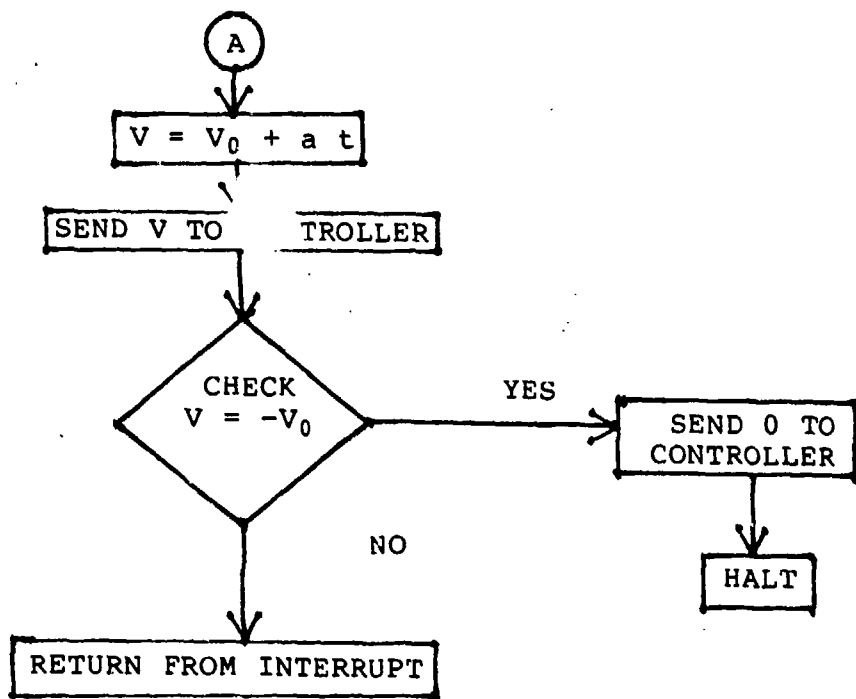
Figure A.2   Interrupt Handler Flow Chart (Continued)

```
                                         TITLE   VELOCITY CONTROLLER     RAY SHEEN
                                         .Z80
                                 ;       SKIP TO EXECUTABLE CODE
    0000'   C3 009A'                     JP INIT
    0003'   00                           NOP
    0004'   00                           NOP
    0005'   00                           NOP
    0006'   00                           NOP
    0007'   00                           NOP
                                 ;
                                 ;       INTERRUPT VECTOR TABLE
                                 ;
    0008'   0000            TABLE:   DW      0          ;NOT USED
    000A'   0010'                    DW      TRAJ       ;CHANNEL 1 INTERRUPT HANDLER
    000C'   0000                     DW      0          ;NOT USED
    000E'   0000                     DW      0          ;NOT USED
                                 ;
                                 ;       VARIABLE LIST
                                 ;
    2100            ZERO     EQU     2100H      ;MOTOR ZERO     <81H>
    2101            VINIT    EQU     2101H      ;INITIAL VELOCITY <54H> (RPM/1000)*25
    2102            ACCEL    EQU     2102H      ;ACCELERATION TIME <40> MSEC*(200/1000)
    2103            CONST    EQU     2103H      ;ACCELERATION DUE TO GRAVITY
    2104            TIME     EQU     2104H      ;TIME COUNTER    200 HZ
    2105            STATE    EQU     2105H      ;STATE VARIABLE
    2106            DUMMY1   EQU     2106H      ;16 BIT DUMMY VARIABLE
    2108            MAG      EQU     2108H      ;MAGNET RELEASE SEQUENCER
                                 ;
                                 ;       CHANNEL #1 INTERRUPT HANDLER
                                 ;
    0010'   3A 2104        TRAJ:    LD A,(TIME)     ;GET THE TIME COUNTER
    0013'   3C                      INC A           ;INCREMENT
    0014'   32 2104                 LD (TIME),A     ;SAVE THE NEW TIME
    0017'   4F                      LD C,A
    0018'   3A 2108                 LD A,(MAG)      ;GET MAGNET RELEASE COUNTER
    001B'   3D                      DEC A           ;DECREMENT IT
    001C'   32 2108                 LD (MAG),A      ;SAVE IT
    001F'   20 09                   JR NZ,AAA       ;IF NOT TIME YET THEN GO
    0021'   3E FF                   LD A,0FFH       ;MAGNET RELEASE
    0023'   D3 9F                   OUT (9FH),A     ;RELEASE MAGNET
    0025'   3E 01                   LD A,1          ;RESET COUNTER
    0027'   32 2108                 LD (MAG),A      ;SAVE IT
    002A'   3A 2105        AAA:     LD A,(STATE)    ;GET STATE VARIABLE
    002D'   FE 01                   CP 01H          ;COMPARE IT TO 1
    002F'   28 18                   JP Z,RUN        ;IF ITS 1 THEN JUMP
    0031'   3A 2102                 LD A,(ACCEL)    ;GET ACCEL
```

106

```
0034'   B9                        CP C              ;CHECK AGAINST CURRENT TIME
0035'   20 05                     JR NZ,CONT        ;IF NOT SAME THEN CONTINUE
0037'   3E 01                     LD A,01H
0039'   32 2105                   LD (STATE),A      ;SAVE THE STATE AS 1
003C'   3A 2101          CONT:    LD A,(VINIT)      ;GET INITIAL VELOCITY
003F'   47                        LD B,A            ;SWITCH REGISTERS
0040'   3A 2100                   LD A,(ZERO)       ;GET THE MOTOR ZERO OFFSET
0043'   80                        ADD A,B           ;ADD OFFSET
0044'   D3 9E                     OUT (9EH),A       ;SEND IT
0046'   FB                        EI                ;ENABLE INTERRUPTS
0047'   ED 4D                     RETI              ;RETURN
                         ;
0049'   21 2106          RUN:     LD HL,DUMMY1      ;ADDRESS OF MULTIPLICATION RESULT
004C'   01 2103                   LD BC,CONST       ;ADDRESS OF CONSTANT
004F'   11 2104                   LD DE,TIME        ;ADDRESS OF TIME
0052'   CD 00C1'                  CALL MULT         ;MULTIPLY THEM
0055'   7E                        LD A,(HL)         ;GET LOW BYTE OF RESULT
0056'   23                        INC HL            ;ADDRESS OF HIGH BYTE
0057'   46                        LD B,(HL)         ;GET HIGH BYTE OF RESULT
                         ;        DIVIDE BY 128
0058'   CB 38                     SRL B
005A'   1F                        RRA
005B'   CB 38                     SRL B
005D'   1F                        RRA
005E'   CB 38                     SRL B
0060'   1F                        RRA
0061'   CB 38                     SRL B
0063'   1F                        RRA
0064'   CB 38                     SRL B
0066'   1F                        RRA
0067'   CB 38                     SRL B
0069'   1F                        RRA
006A'   CB 38                     SRL B
006C'   1F                        RRA
006D'   47                        LD B,A            ;SWITCH REGISTERS
006E'   CB 78                     BIT 7,B           ;CHECK IF IT'S NEGATIVE
0070'   20 06                     JR NZ,ADDEM       ;IF NOT CHANGE IT
0072'   3E D0                     LD A,11010000B    ;158 OR 2*104
0074'   90                        SUB B             ;FIND THE DIFFERENCE
0075'   ED 44                     NEG               ;GET THE 2'S COMPLEMENT
0077'   47                        LD B,A            ;SAVE IT
0078'   3A 2101          ADDEM:   LD A,(VINIT)      ;GET INITIAL VELOCITY
007B'   80                        ADD A,B           ;ADD EM
007C'   4F                        LD C,A            ;SAVE IN C REGISTER
007D'   3A 2100                   LD A,(ZERO)       ;GET OFFSET FOR D TO A
0080'   81                        ADD A,C           ;ADD OFFSET
```

107

```
0081'    D3 9E                         OUT (9EH),A      ;SEND IT
                                  ;
                                  ;       SEE IF IT'S FINISHED
                                  ;
0083'    3A 2101                       LD A,(VINIT)     ;GET VINIT
0086'    C6 08                         ADD A,8          ;HIGHER VELOCITY BECAUSE OF LAG
0088'    ED 44                         NEG              ;2'S COMPLEMENT OF VINIT
008A'    39                            CP C             ;COMPARE THEM
008B'    28 03                         JR Z,STOP        ;IF EQUAL, THEN STOP
008D'    FB                            EI               ;ENABLE INTERRUPTS
008E'    ED 4D                         RETI             ;RETURN
                                  ;
                                  ;       STOP IT
                                  ;
0090'    3A 2100            STOP:      LD A,(ZERO)      ;MOTOR ZERO
0093'    D3 9E                         OUT(9EH),A       ;SEND IT
0095'    3E 80                         LD A,80H         ;MAGNET ON
0097'    D3 9F                         OUT (9FH),A
0099'    76                            HALT             ;STOP THE PROGRAM
                                  ;
                                  ;       PROGRAM INITIALIZATION
                                  ;
009A'    3E 00              INIT:      LD A,00H
009C'    32 2104                       LD (TIME),A      ;SET TIME TO ZERO
009F'    32 2105                       LD (STATE),A     ;SET STATE VARIABLE
00A2'    3E 80                         LD A,80H         ;MAGNET ON VALUE
00A4'    D3 9F                         OUT (9FH),A      ;TURN MAGNET ON
00A6'    3E 98                         LD A,10011000B   ;GRAVITY CONSTANT -104
00A8'    32 2103                       LD (CONST),A     ;SET CONST
                                  ;
                                  ;       SET CTC CHANNEL
                                  ;
00AB'    21 0008'                      LD HL,TABLE      ;INTERRUPT VECTOR TABLE ADDRESS
00AE'    7C                            LD A,H           ;GET HIGH BYTE
00AF'    ED 47                         LD I,A           ;STORE IT
00B1'    7D                            LD A,L           ;GET LOW BYTE
00B2'    D3 84                         OUT (84H),A      ;SEND IT
00B4'    3E A7                         LD A,10100111B   ;CONTROL WORD FOR CTC
                                  ;
                                  ;       BIT 7 - ENABLE INTERRUPT
                                  ;       BIT 6 - USE INTERNAL CLOCK
                                  ;       BIT 5 - CLOCK AT 7800 HZ
                                  ;       BIT 4 - DISREGARD
                                  ;       BIT 3 - START COUNTING NOW
                                  ;       BIT 2 - TIME CONSTANT FOLLOWS
                                  ;       BIT 1 - ZERO CHANNEL
```

```
                                    ;       BIT 0 - MUST BE 1
                                    ;
00A6'   D3 85                               OUT (85H),A         ;SEND IT
00A8'   3E 27                               LD A,39             ;TIME CONSTANT FOR 200 HZ
00AA'   D3 85                               OUT (85H),A         ;SEND IT
00AC'   ED 5E                               IM 2                ;INTERRUPT MODE 2
00AE'   FB                                  EI                  ;ENABLE INTERRUPTS
                                    ;
00BF'   18 FE               LOOP:   JR LOOP                     ;GO FOREVER
                                    ;
                                    ;       MULTIPLICATION SUBROUTINE
                                    ;
00C1'   F5                  MULT:   PUSH AF             ;SAVE REGISTERS
00C2'   C5                          PUSH BC
00C3'   D5                          PUSH DE
00C4'   0A                          LD A,(BC)           ;FETCH ARG 1
00C5'   47                          LD B,A
00C6'   1A                          LD A,(DE)           ;FETCH ARG 2
00C7'   4F                          LD C,A
00C8'   AF                          XOR A               ;CLEAR ACCUMULATOR
00C9'   57                          LD D,A
00CA'   1E 08                       LD E,8              ;SET LOOP COUNTER
00CC'   CB 40               MULT2:  BIT 0,B             ;WE'RE AT ZERO, DO WE STAY THERE
00CE'   28 01                       JR Z,MULT3          ;IF SO, JUST SHIFT AROUND
00D0'   91                          SUB C               ;ELSE SUBTRACT ARG 2 FROM PRODUCT
00D1'   CB 2F               MULT3:  SRA A               ;SHIFT PRODUCT RIGHT
00D3'   CB 1A                       RR D
00D5'   1D                          DEC E               ;DECREMENT LOOP COUNTER
00D6'   28 15                       JR Z,MULT5          ;BAIL OUT IF DONE
00D8'   CB 38                       SRL B               ;ROTATE ARG 1 RIGHT
00DA'   30 F0                       JR NC,MULT2         ;IF NEXT BIT IS ZERO, BRANCH
00DC'   CB 40               MULT4:  BIT 0,B             ;IF WE'RE AT 1 DO WE STAY THERE
00DE'   20 F1                       JR NZ,MULT3         ;IF SO JUST SHIFT PRODUCT
00E0'   81                          ADD A,C             ;ELSE ADD ARG 2 TO PRODUCT
00E1'   CB 2F                       SRA A               ;SHIFT PRODUCT RIGHT
00E3'   CB 1A                       RR D
00E5'   1D                          DEC E               ;DECREMENT LOOP COUNTER
00E6'   28 05                       JR Z,MULT5          ;BAIL OUT IF DONE
00E8'   CB 38                       SRL B               ;ROTATE ARG 1 RIGHT
00EA'   C3 00CC'                    JP MULT2            ;DO IT AGAIN
00ED'   72                  MULT5:  LD (HL),D           ;SAVE PRODUCT
00EE'   23                          INC HL
00EF'   77                          LD (HL),A
00F0'   2B                          DEC HL
00F1'   D1                          POP DE              ;RECOVER REGISTERS
00F2'   C1                          POP BC
```

109

```
00F3'   F1                              POP AF
00F4'   C9                              RET
                                ;
                                ;       THAT'S ALL FOLKS
                                ;.
                                        END
```

APPENDIX B

GRAPHITE/EPOXY LAYERING SEQUENCE AND CURING CYCLE

The stacking sequence for the curing cycle of graphite/epoxy laminates is shown below:

top plate

1.

5.

4.

2.

3.

2.

1.

cure plate
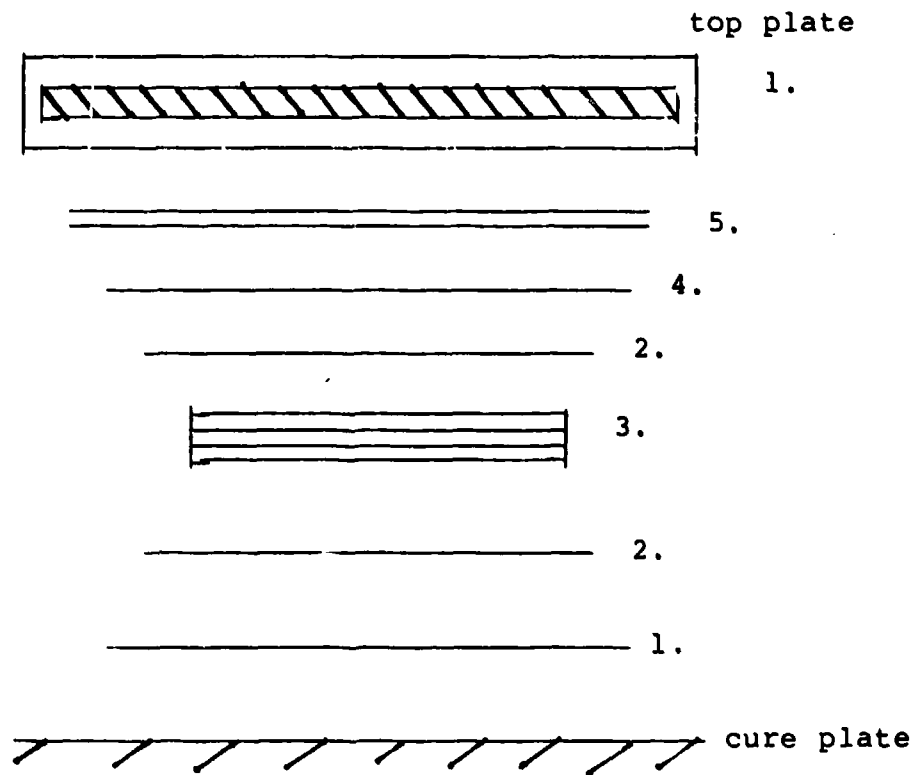
1. Guaranteed non-porous teflon
2. Peel ply
3. Laminate
4. Porous teflon
5. Bleeder paper

Figure B.1 Stacking Sequence

The curing cycle was as follows:

Time (min.)	Vacuum (psi)	Ext. Pressure (psi)	Total Pressure (psi)	Temp. (°F)
0	14.7	0	14.7	100
20	14.7	85	100	110
35	14.7	85	100	240
95	14.7	85	100	240
110	14.7	85	100	350
230	14.7	85	100	350
250	14.7	85	100	160
255	0	0	0	75

Appendix C

STRAIN LEVEL DETERMINATION

Consider the Wheatstone Bridge Circuit where initially $\Delta R = 0$.
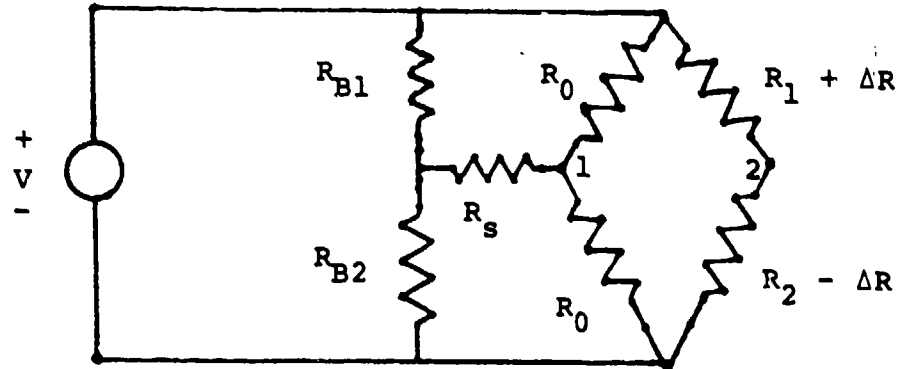

Figure C.1   Wheatstone Bridge Circuit

R_s, R_{B1}, and R_{B2} can be varied to ensure the potential between nodes 1 and 2 is initially zero.

so

$$V_0 = V_1 - V_2 = 0 \tag{C.1}$$

therefore

$$V_1 = V_2 \tag{C.2}$$

but

$$V_2 = \frac{R_1}{R_1 + R_2} \, V \tag{C.3}$$

since

$$\Delta R = 0$$

then

$$V_1 = \frac{R_1}{R_1 + R_2} \, V \tag{C.4}$$

113

Now as ΔR becomes non zero

$$V_2 = \frac{R_1 + \Delta R}{R_1 + R_2} V \qquad (C.5)$$

so $\qquad V_0 = V_1 - V_2 = \frac{R_1}{R_1 + R_2} V - \frac{R_1 + \Delta R}{R_1 + R_2} V \qquad (C.6)$

or $\qquad V_0 = -\frac{\Delta R}{R_1 + R_2} V \qquad (C.7)$

we define $R_1 = R_2 = R$

so $\qquad V_0 = -\frac{\Delta R}{2R} V \qquad (C.8)$

From the definition of gauge factor

$$GF \equiv \frac{\Delta R/R}{\Delta L/L} = \frac{\Delta R}{R\epsilon} \qquad (C.9)$$

where ϵ is the strain level.

Substituting equation C.9 into equation C.8 gives

$$V_0 = -\frac{GF \epsilon}{2} V \qquad (C.10)$$

if V_0 is amplified by a gain, A, the relationship between V_{amp} and the strain level, ϵ is

$$V_{AMP} = -\frac{A V GF}{2} \epsilon \qquad (C.11)$$

114

APPENDIX D

DERIVATION OF ZENER EQUATION

Assuming a metal behaves as according to Zener's theory, we can write the following relationship for stress and strain.

$$a_1 \sigma + a_2 \dot{\sigma} = b_1 \epsilon + b_2 \dot{\epsilon} \qquad (D.1)$$

If Eq. (D.1) is divided by a_1, three new independent constants are introduced.

$$\sigma + \tau_\epsilon \dot{\sigma} = E_R (\epsilon + \tau_\sigma \dot{\epsilon}) \qquad (D.2)$$

Where the relaxed modulus, E_R, is equivalent to the static Young's Modulus, E. The τ's are the relaxation times for stress and strain.

Now suppose both ϵ and $\dot{\epsilon}$ are equal to zero, then Eq. (D.2) reduces to

$$\sigma + \tau_\epsilon \dot{\sigma} = 0 \qquad (D.3)$$

115

which has the solution

$$\sigma(t) = \sigma_0 \, e^{-t/\tau_\epsilon} \tag{D.4}$$

Similarly, if σ and $\dot{\sigma}$ are set equal to zero, the solution to Eq. (D.2) reduces to

$$\epsilon(t) = \epsilon_0 \, e^{-t/\tau_\sigma} \tag{D.5}$$

Equations (D.4) and (D.5) show that stress and strain exponentially approach equilibrium conditions.

Now suppose that in a very short time interval, Δt, a solid receives a finite stress increment $\Delta\sigma$, and therefore a finite strain increment $\Delta\epsilon$. Then Eq. (D.2) becomes

$$\Delta\sigma \, \Delta t + \tau_\epsilon \frac{\Delta\sigma}{\Delta t} \, \Delta t = E_R \left(\Delta\epsilon \, \Delta t + \tau_\sigma \frac{\Delta\epsilon}{\Delta t} \, \Delta t \right) \tag{D.6}$$

Now integrate (D.6) and let Δt approach zero. As Δt approaches zero the first expression on each side of (D.6) goes to zero. The integral becomes

$$\tau_\epsilon \, \Delta\sigma = E_R \, \tau_\sigma \, \Delta\epsilon \tag{D.7}$$

or,

$$\Delta \sigma = E_u \, \Delta \epsilon \qquad (D.8)$$

Where E_u is called the unrelaxed elastic modulus, defined by

$$E_u = E_R \, \frac{\tau_\sigma}{\tau_\epsilon} \qquad (D.9)$$

If however, stress and strain are cyclically loaded, or if the solid is undergoing free vibration, then

$$\sigma(t) = \sigma_0 \, e^{i\omega t} \qquad (D.10a)$$

$$\epsilon(t) = \epsilon_0 \, e^{i\omega t} \qquad (D.10b)$$

Placing (D.10) into (D.2) gives

$$(1 + i\omega\tau_\epsilon) \, \sigma_0 = E_R \, (1 + i\omega\tau_\sigma)\epsilon_0 \qquad (D.11)$$

Rearranging gives

$$\sigma_0 = E_R \, \frac{1 + i\omega\tau_\sigma}{1 + i\omega\tau_\epsilon} \, \epsilon_0 \qquad (D.12)$$

117

or

$$\sigma_0 = E_C \, \epsilon_0 \qquad \text{(D.13)}$$

where

$$E_C = E_R \left(\frac{1 + i\omega\tau_\sigma}{1 + i\omega\tau_\epsilon} \right) \qquad \text{(D.14)}$$

E_C is defined as the complex modulus.

Separating (D.14) into real and imaginary parts gives

$$E_C = \left(\frac{1 + \omega^2 \tau_\epsilon \tau_\sigma}{1 + \omega^2 \tau_\epsilon^2} + i \, \frac{\omega\tau_\sigma - \omega\tau_\epsilon}{1 + \omega^2 \tau_\epsilon^2} \right) E_R \qquad \text{(D.15)}$$

From Eq. (D.13) it can be shown that strain lags behind stress. This lag is a function of frequency, and the relaxation coefficients τ_σ and τ_ϵ. The angle which strain lags behind stress is defined as δ. The tangent of δ is called the damping factor, g, and is equal to the imaginary part of the complex modulus. The damping ratio, ζ, is one half the value of g.

118

$$E_C = E_R' (1 + i\,g) \qquad (D.16)$$

$$\tan \delta = g = \frac{\text{Im }[E_C]}{\text{Re }[E_C]} \qquad (D.17)$$

$$g = \frac{\omega(\tau_\sigma - \tau_\epsilon)}{1 + \omega^2(\tau_\epsilon\,\tau_\sigma)} \qquad (D.18)$$

Define $\bar{\tau}$ as the geometric mean of the two relaxation times.

$$\bar{\tau} = (\tau_\epsilon\,\tau_\sigma)^{1/2} \qquad (D.19)$$

Define $\bar{E}$ as the geometric mean of the two moduli E_u and E_R.

$$\bar{E} = (E_u\,E_R)^{1/2} \qquad (D.20)$$

Placing Eqs. (D.19) and (D.20) into (D.18) gives

$$g = \frac{E_u - E_R}{\bar{E}} \left(\frac{\omega\bar{\tau}}{1 + \omega^2\,\bar{\tau}^2} \right) \qquad (D.21)$$

119

Thus, we can see the relationship between damping ratio, ζ, and frequency. Equation (D.21) is presented in Chapter IV as

$$\zeta = \frac{g}{2} = \frac{(\alpha^2 \text{ ET})}{2c} \left(\frac{\omega\tau}{1 + \omega^2 \tau^2} \right) \qquad (D.22)$$

where

$$\frac{E_u - E_R}{\bar{E}} = \frac{\alpha^2 \text{ ET}}{c} \qquad (D.23a)$$

$$\bar{\tau} = \tau \qquad (D.23b)$$

Equation (D.23a) is derived using thermodynamic properties of metals. See Ref. 5 for the derivation of this equation.

120